
Towards operational satellite based atmospheric monitoring in Norway SatMoNAir

Final project report

Kerstin Stebel, Aasmund Fahre Vik, Cathrine Lund Myhre,
Ann Mari Fjæraa, Tove Svendby and Phillip Schneider



Scientific report

Preface

The SatMoNAir project [NSC contract nr. JOP.12.12.2] builds on a previous NRS 'følgemiddel' project, called 'Roadmap towards EarthCARE and Sentinel 5 precursor', within which NILU and met.no developed a strategy and concrete plans for how best to prepare themselves for future European satellite missions for measuring atmospheric composition, with respect to their national monitoring, weather predictions and research tasks. A range of possible applications and tasks were suggested by both institutes. Three tasks were considered to be particularly relevant to pursue in the near future and these are brought forward in a proposal for 'følgemidler' in 2012 by NILU. The selection of task was done based on three aspects: (1) What was considered to be mature enough to follow up now (e.g. methane measured from space is not mature enough for operational monitoring use), (2) what would have the largest impact on the routinely NILU operation (what will be important for national and international monitoring tasks) and (3) what would be feasible to accomplish without a large research activity.

The long-term goal of the proposed activity is to be ready to utilize operational data for routine monitoring, especially that provided by the Sentinel 5 precursor mission. To get there, it is suggested to work with similar types of data from existing satellites to test feasibility of the data products and to establish methodologies, tools, maps and time-series of data that can then be continued once the operational missions are available.

The outcomes of the SatMoNAir project, obtained during the project period between 01.01.2012 and 28.02.2013, are summarized in this report.

Contents

	Page
Preface	1
Summary	5
1 Aerosols – Climate effects in Scandinavia and polar regions: analysis of episodes with high aerosol loads for KLIF reporting (WP 1).....	7
1.1 National monitoring of climate gases and selected aerosol properties.....	7
1.2 Aerosols.....	8
1.3 Trace gases	12
1.4 References	18
2 Use of satellite based ozone measurements in national reporting (WP 2).....	20
2.1 Monitoring of the atmospheric O ₃ layer and UV radiation	20
2.2 Satellite ozone measurements	20
2.3 Satellite based time-series of ozone	22
2.4 Analysis and reporting	24
2.5 References	24
3 Satellite based Air Quality monitoring of remote areas for EMEP reporting (WP 3).....	25
3.1 Introduction	25
3.2 Methodology	25
3.3 Results	29
3.3.1 Long-term average Mapping.....	30
3.3.2 Product inter-comparison	32
3.3.3 Time series	37
3.4 Conclusions	43
3.5 References	44
Appendix A Glantz et al., poster, CRAICC meeting, 2012	47
Appendix B Chapter 6.5 of Myhre et al. (2012).....	51
Appendix C Chapter 5.1 of Myhre et al. (2012)	59
Appendix D Chapter 4 of Svendby et al. (2012)	63

Summary

The SatMoNAir project [NSC contract nr. JOP.12.12.2] builds on a previous NRS 'følgemiddel'-project, called 'Roadmap towards EarthCARE and Sentinel 5 precursor', within which NILU and met.no developed a strategy for how best to prepare themselves for future European satellite missions for measuring atmospheric composition, with respect to their national monitoring, weather predictions and research tasks. Three specific topics were considered particularly relevant: a. Aerosols – Climate effects in Scandinavia and polar regions: analysis of episodes with high aerosol loads should be included in the annual report to the Norwegian Environment Agency (the former KLIF), b. Use of satellite based ozone measurements in national reporting, and c. Satellite based Air Quality monitoring of remote areas for EMEP reporting. Results from the work performed are described in this report. The outcomes of the project have been utilized in support of the National monitoring of greenhouse gases and aerosols (see Myhre et al., 2012), the atmospheric ozone layer (see Svendby et al., 2012), and have been reported to EMEP.

Towards operational satellite based atmospheric monitoring in Norway SatMoNAir

Final project report

1 Aerosols – Climate effects in Scandinavia and polar regions: analysis of episodes with high aerosol loads for KLIF reporting (WP 1)

The work has focused on two aspects of aerosols: a. direct observations of aerosols (in terms of total column measurements (AOD) and their vertical distribution) and b. carbon monoxide (CO), which is a tracer for aerosols from biomass burning. The results have been utilized to improve the Monitoring of greenhouse gases and aerosols at Svalbard and Birkenes, which NILU is performing on behalf of the Norwegian Environment Agency.. The results obtained have been reported in dedicated chapters in the annual reports to Klif in 2012 (Myhre et al., 2012). A follow up will be included in the report, which will be submitted to the Norwegian Environment Agency in November 2013.

1.1 National monitoring of climate gases and selected aerosol properties

In 1999 The Norwegian Environment Agency (former Klif) and NILU signed a contract where NILU is commissioned to run a programme for monitoring of greenhouse gases at the Zeppelin station, close to Ny-Ålesund at Svalbard. This collaborative Klif/NILU programme includes monitoring of 23 greenhouse gases at the Zeppelin observatory in the Arctic. In 2009 NILU upgraded and extended the observational activity at the Birkenes Observatory in Aust-Agder and in 2010 the monitoring programme was extended to also include the new observations from Birkenes of the greenhouse gases CO₂ and CH₄ and selected aerosols relevant for the understanding of climate change. The purpose of the programme is to:

- Provide continuous measurements of greenhouse gases in the Arctic region and at Birkenes resulting in high quality data that can be used in trend analysis
- Provide trend analysis and interpretations of the observations from Zeppelin to assess the influence regional anthropogenic emissions of greenhouse gases has on the radiative balance
- Provide information on the status and the development of the greenhouse gases with a particular focus on the gases included in the international conventions (the Montreal and Kyoto protocols)
- Provide results of aerosol observations of relevance to the understanding of climate change
- Indicate source regions with high influence on the measurements.

Monitoring of aerosol optical depth ADO above Ny-Ålesund, established in 2002 as one of the 12 GAW station PFR-sun-photometer network, is an integrated part of the climate gas monitoring programme, new aerosol observations from the

Birkenes observatory were included in the monitoring programme for the first time in 2009.

In total, NILU operates three atmospheric observatories, one each at Zeppelin Mountain and Ny-Ålesund, Svalbard, at Birkenes in Southern Norway, and at Troll Station, Queen Maud Land, in Antarctica. The aerosol variables observed at these stations follows the GAW recommendations. The variables have been selected for their relevance to assessing the aerosol climate effect, for their feasibility of being operated long-term with manageable maintenance, and for synergy aspects with air quality and health effect questions.

1.2 Aerosols

Despite relative high uncertainties of satellite aerosol products in the Arctic, the use of earth-observation (EO) data in polar region is steadily increasing.

Huge emissions from boreal forest fires in North America, with light absorbing aerosol containing BC, were transported into the Arctic region and very likely explain the elevated AOD levels end of July 2004. Stohl et al. (2006) used MODIS images and MODIS fire detections products for their study. Agricultural fires in Eastern Europe resulted in elevated pollution levels in the Arctic in spring 2006. Stohl et al. (2007) and Myhre et al. (2007) found that these aerosols had a strong cooling effect on the Arctic during this period, with a moderate warming effect when the aerosol layer were above snow covered surface areas. Also this studies included Earth Observation data: MODIS images, fire detections, and AOD (MODIS Collection Version 5), as well as CO columns retrieved from AIRS data. Another example for utilization of EO data in the Arctic, is the work from Sodemann et al. (2011), describing episodes of cross-polar transport in the Arctic troposphere during July 2008 as seen from models, satellite, and aircraft observations. The authors use CO from the IASI passive infrared sensor on-board the MetOp-A satellite and aerosol backscatter and depolarization from the CALIPSO satellite. Kristiansen et al. (2010) use SO₂ columns from GOME-2, OMI, and AIRS, and total attenuated backscatter at 532 nm and 1064 nm (level 1B data) from CALIOP, to study the transport of the Kasatochi (52.2°N, 175.5°W) eruption sulphur dioxide cloud on 7 to 8 August 2008, leading to an increase of total aerosol column above Ny-Ålesund in August and September 2008.

For a long time there have been relative few systematic observations of Arctic aerosols based on Earth Observation data alone, but many global and European studies cover the area of Southern Scandinavia (e.g. Myhre et al., 2005, Schaap et al., 2008, Glantz et al., 2009). More recently, retrievals have been developed for spectral AOD over snow, in the Arctic regions, using AATSR data in the visible (Istomina et al., 2009) and infrared regions (Istomina et al., 2011), as well as MODIS (Mei et al., 2013). A comparison of AOD in the Arctic with model, satellite and ground-based data has been published by von Hardenberg et al. (2012). This study includes a comparison to Scandinavian sun-photometer sites (Ny-Ålesund, ALOMAR, and Sodankylä), but only a very incomplete ground-based dataset was used for comparison (a couple of seasons), despite the existence of much longer time series. In 2013, Di Pierro et al. (2013) and Winker et al. (2013) reported the 3-D distribution of tropospheric aerosols as characterized by

CALIOP onboard of CALIPSO. CALIOP aerosol records mainly cover the occurrence of enhanced aerosol loadings; typical background aerosol loadings in the Arctic are below the detection limit of the LIDAR.

We have performed an initial evaluation of AOD products distributed through the ESA Aerosol-CCI project (see www.esa-aerosol-cci.org), using the round-robin dataset from 2008. Standard AOD data are not particularly tuned to be usable in the Arctic region, often a cutoff is set at around 70°N and no data are available for the region around Svalbard. As an example for a rough assessment of the suitability of the CCI aerosol retrievals for the Norwegian National monitoring, in Figure 1, monthly mean AOD values at 550 nm from the AATSR ORAC v. 2.02 retrieval are given. The typical overestimation above snow-covered areas during winter-time, for example over the Russian sea and the high plateau of Greenland is clearly seen.

Despite this overestimation in the Arctic region, the dataset might still add valuable information to the Norwegian national monitoring complementary to the existing ground-based observations.

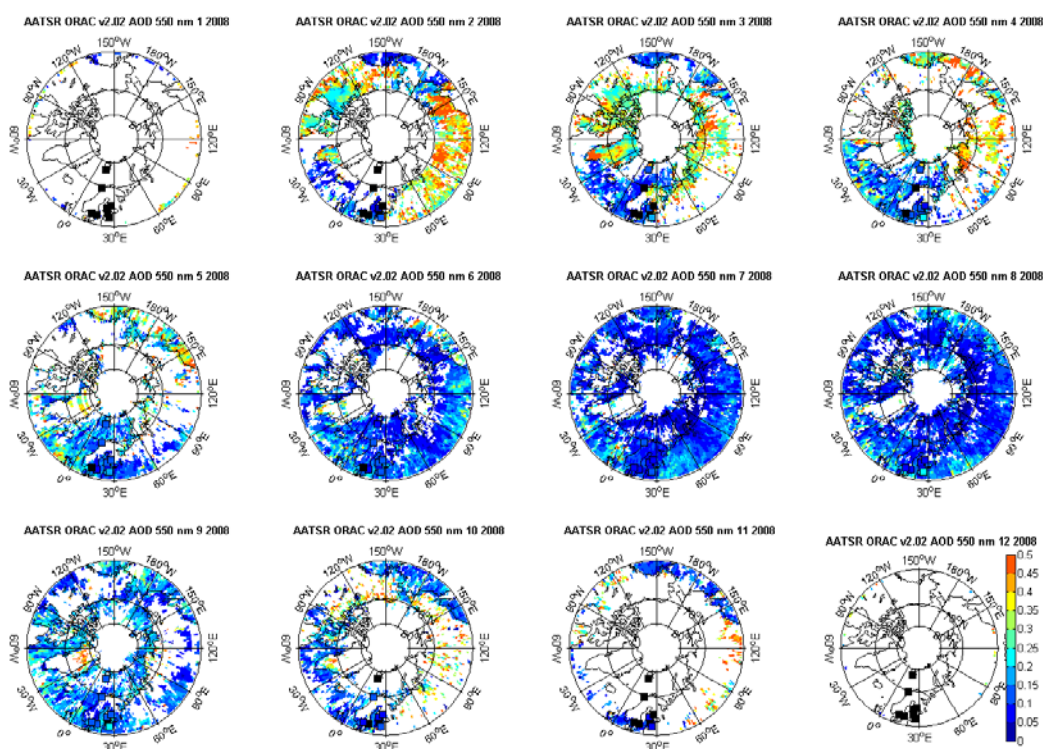


Figure 1: Monthly averages of AATSR ORAC v2.02 data for 2008.

An overview all ground-based sun photometer sites in the European Arctic sector and Scandinavia has been given by Toledano et al (2012), see Table 1. In Figure 2 we show the monthly averaged data from AATSR ORAC v. 2.02 and the AOD observations from the ground-based AERONET network. Due to lack of sun, no data are available for the month of January and December 2008. An initial comparison between daily data shows reasonable correlations, for example 0.52 for Ny-Ålesund and 0.66 for Palgrunden. It is obvious that the satellite data are

adding the spatial information not covered by ground-based observations from Ny-Ålesund and Birkenes (started in 2009), which are the two sites at present funded via KLIF's monitoring programme. Nevertheless, further analysis is needed to assess the added value of these observations in a more quantitative way. Also, further analysis is important to assess whether the satellites correctly describe inter-annual variability and trends, which is a task in the SatMonAir-II project in 2013.

Table 1: List of sun photometer sites in the European Arctic sector and Scandinavia.

Site	Institution	Coordinates	Network	Instrument	Start	End
Hornsund	GSFC,PAN	77.0°N, 15.6°E	AERONET	Cimel	2004	–
Longyearbyen	GSFC	78.2°N, 15.6°E	AERONET	Cimel	2003	2004
Ny_Ålesund	AWI	78.9°N, 11.9°E	Polar-AOD	SP1A	1991	–
Ny_Ålesund	NILU,WRC	78.9°N, 11.9°E	GAW-PFR	PFR	2002	–
Andenes	UVA,NILU,ARR	69.3°N, 16.0°E	AERONET-RIMA	Cimel	2002	–
Kiruna	SMHI	67.8°N, 20.4°E	GAW-PFR	PFR	2007	–
Sodankylä	FMI	67.4°N, 26.6°E	GAW-PFR	PFR	2004	–
Birkenes	NILU, UVA	58.4°N, 8.3°E	AERONET-RIMA	Cimel	2009	–
Gotland	SMHI	57.9°N, 19.0°E	AERONET	Cimel	1999	2004
Gustav_Dalen_Tower	JRC	58.6°N, 17.5°E	AERONET	Cimel	2005	–
Helsinki	FMI	60.2°N, 25.0°E	AERONET	Cimel	2008	–
Helsinki_Lighthouse	JRC, FIMR	59.9°N, 24.9°E	AERONET	Cimel	2006	–
Hyytiälä	FMI	61.8°N, 24.3°E	AERONET	Cimel	2008	–
Jokioinen	FMI	60.8°N, 23.5°E	GAW-PFR	PFR	2004	–
Kuopio	FMI	62.9°N, 27.6°E	AERONET	Cimel	2008	–
Norrköping_1995	SMHI	58.6°N, 16.2°E		SPM2000	1995	–
Norrköping	SMHI,ESA,SNSB	58.6°N, 16.2°E	GAW-PFR	PFR	2007	–
Palgrunden	ESA, SU, SNSB	58.8°N, 13.2°E	AERONET	Cimel	2008	–
SMHI ^a	SMHI	58.6°N, 16.2°E	AERONET	Cimel	2001	2006
Visby	SMHI	57.7°N, 18.4°E	GAW-PFR	PFR	2007	–

^a The Norrköping station was AERONET site under the name 'SMHI'.

In collaboration with the University Stockholm work has been performed related to aerosol optical density (AOD) measurements around Svalbard (see attached poster by Glantz et. al. (2012) given as Annex A). An example is shown in Figure 3: MODIS Aqua scenes of AOT at 555 nm for two overpasses is given a) in summer and b) in spring, illustrating the low aerosol load in summer and the extreme values in May 2006. The white box in each figure denotes the area (82°N - 75°N, 10°W - 40°E) used for the averaging of MODIS retrieved aerosol optical parameters. Figure 4 shows the general good correlation between MODIS and AERONET/Polar-AOD median column AOT. By introducing MODISc005 retrievals of aerosol optical density (AOD) over the area around Svalbard, substantially better time coverage (~75%), compared to ground-based sun-photometer data (~30%) is obtained for the subarctic marine region. MODISc005 AOD was found to be within 30% of the ground-based estimates and, for values lower than 0.2, on the whole within the expected uncertainty range of MODIS retrievals over ocean surfaces. Short- and long-term variations in AOT will need to be investigated further with better accuracy.

The results from work-package 1 have been included in NILU's 'climate gas' report "*Monitoring of greenhouse gases and aerosols at Svalbard and Birkenes: Annual report 2012*", prepared for KLIF in 2012 (for full report see Myhre et al., 2012). Chapter 6.5, which dealt with Earth Observations of aerosols above Scandinavia, is given as Appendix B.

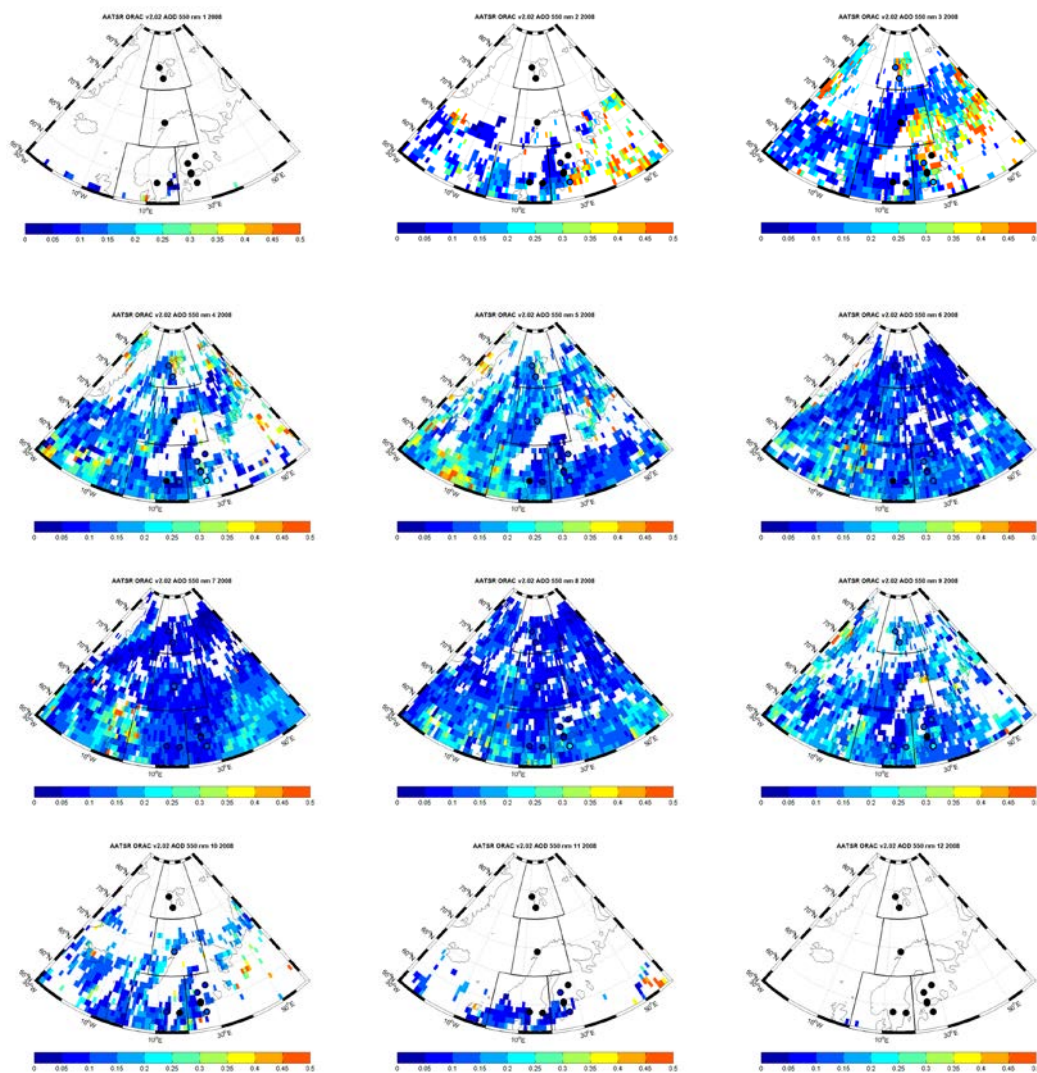


Figure 2: Monthly averaged data from AATSR ORAC v. 2.02 and the AOD observations from the ground-based AERONET network for the Scandinavian Arctic sector. Observations are marked as circles.

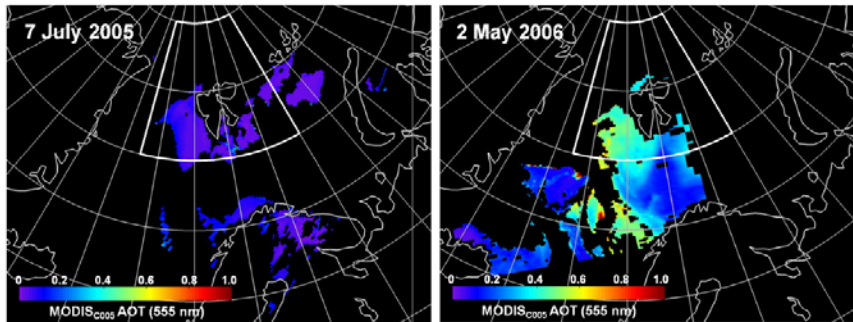


Figure 3: MODIS Aqua scenes of AOT at 555 nm for two overpasses: a) in summer and b) in spring. The white box in each figure denotes the area (82°N - 75°N, 10°W - 40°E) used for the averaging of MODIS retrieved aerosol optical parameters.

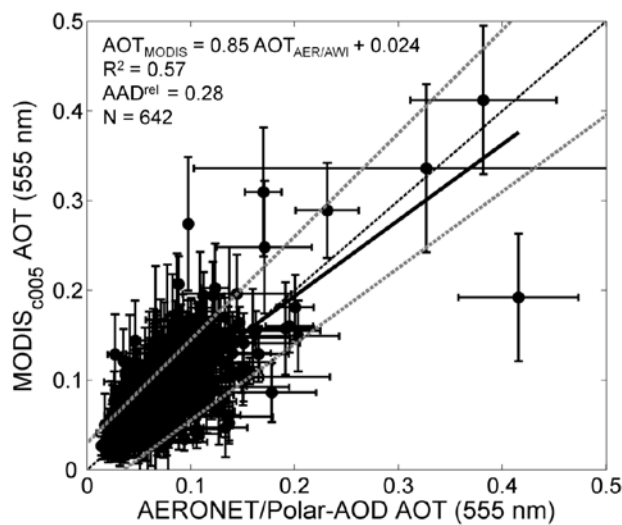


Figure 4: Comparison between MODIS and AERONET/Polar-AOD median column AOT, and corresponding one standard deviation, at 555 nm. The black solid, grey dashed, and black dotted lines represent linear fits of the AOT values, expected uncertainties for one standard deviation of the MODIS aerosol retrievals, and the 1-to-1 line, respectively. Text at the left top describes the expression for the linear regression curve, coefficient of determination (R^2), relative absolute average deviation (AAD^{rel}) and number of matches (N).

1.3 Trace gases

For trace gases and fire products we have investigated the availability of a number of relevant satellite products available online. Carbon monoxide (CO) is a component of particular importance as tracer for aerosols from biomass burning, and ground based monitoring of this compound is lacking in continental Norway. The relevant CO products for various time periods are illustrated in Figure 5.

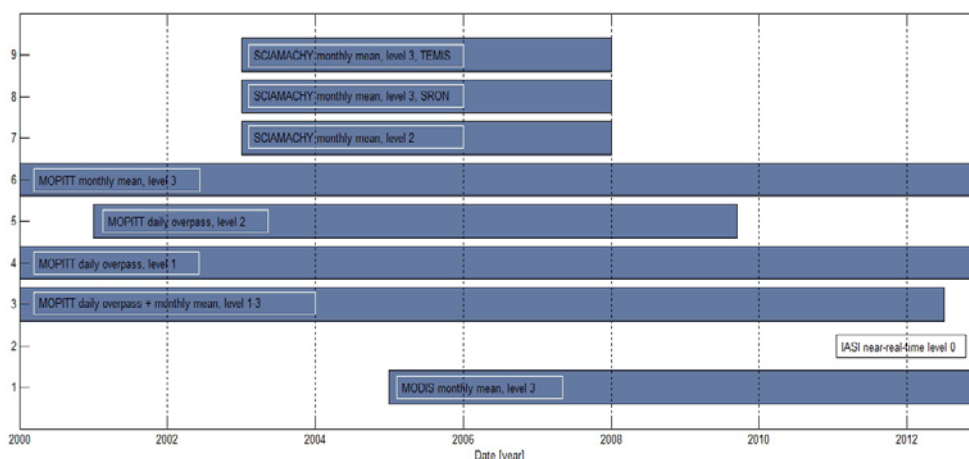


Figure 5: EO-based CO data of particular importance for national monitoring to KLIF.

Not all the above listed products are well suited for our purpose in the SatMoNAir project. The availability of data in time and space does in some cases not cover the region or the years of interest, and while investigating the available products in detail, we also discovered that the routines for searching, online plotting and download of data might not be straight forward.

A simple web page serves as the final report categorising and providing links to the relevant trace gas products. This is set up for internal use at <http://zardoz.nilu.no/~annm/satmonair/> at NILU for easy access and employment of the desired products. The web page contains additional information about the metadata and experiences of the products listed in Figure 5 (e.g. information on satellite/instrument, data level, product type, data period and URL to the online product.)

EO fire products are important for the understanding of ground based aerosol observations and CO. The web page at <http://zardoz.nilu.no/~annm/satmonair/> does not only contain a list of EO products used, but also URLs to online fire products provided by FIRMS (Fire Information for Resource Management System) <http://earthdata.nasa.gov/data/near-real-time-data/firms>. FIRMS does also provide an online e-mail alert service where the user can sign up for receiving e-mail when hot-spots are detected in a user specified area of interest. NILU is subscribed to this service and we receive daily updates from the system. Global fire maps as shown in Figure 6 are available in Near-Real-Time (NRT).

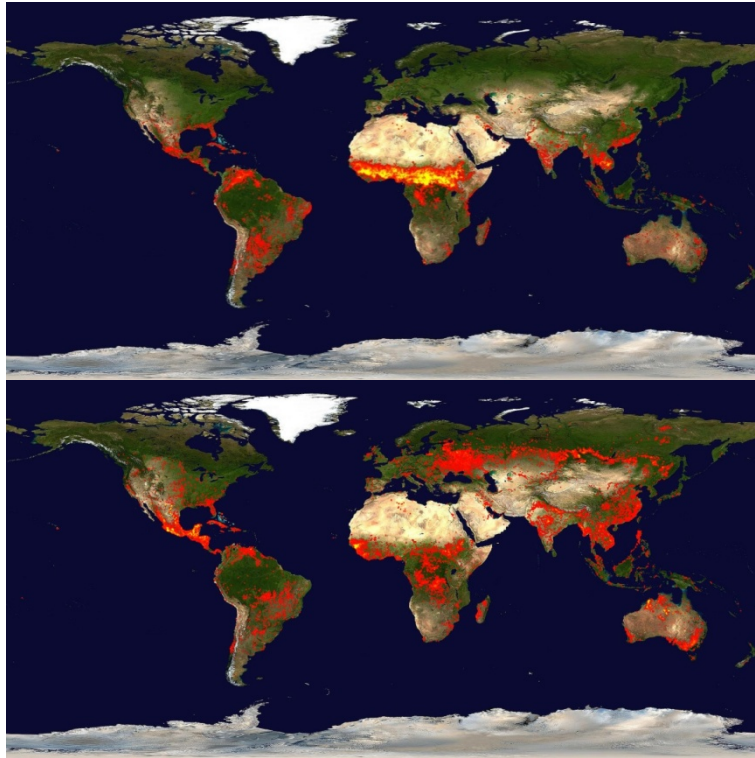


Figure 6: Upper panel: The geographical locations of all hot spots detected by MODIS on 11.-20 January 2011. In the northern hemisphere winter there are very few fires in the Eastern Europe and Russian areas, where we have our focus in SatMonAir. Lower panel: The geographical locations of all hot spots detected by MODIS on 21.-30 May 2011. The northern hemisphere spring is an active season for natural fires in the Eastern Europe and Russian areas.

We have further investigated a few well known high aerosol episodes in the Arctic and Scandinavian areas in the years 2004-2011 with special emphasis on 2011, which was included in the 2012 Klif report. In 2011 there were very few episodes at both Birkenes and Zeppelin, partly due to the meteorology with prevailing winds from west in the spring season.

To identify the episodes of high aerosol loads and above average mixing ratios of trace gases in 2011 we have used *in situ* data from Zeppelin (CO, O₃, black carbon) and Birkenes (CO₂) in combination with the FLEXTRA air mass trajectories. We have also compared the measurements and the air mass trajectories to the global fire maps and to the direct overpass data from MODIS Terra and Aqua and MOPITT.

D22214

STOHL ET AL.: PAN-ARCTIC TRANSPORT OF FIRE AEROSOLS

D22214

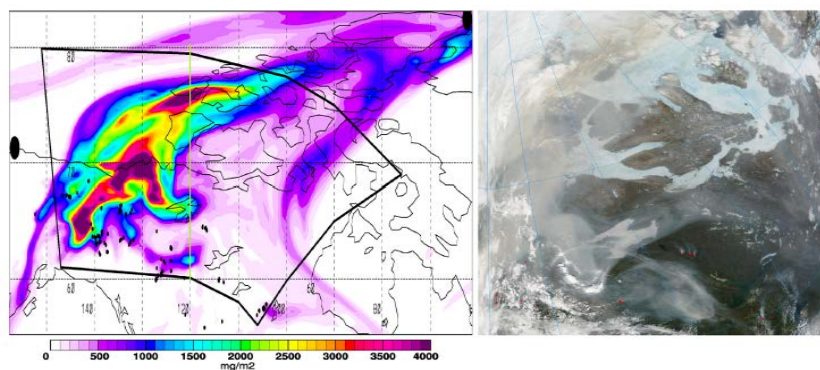


Figure 7. (left) Total columns of the FLEXPART CO tracer at 1800–2100 UTC and (right) MODIS Terra image at 1935 UTC on 5 July 2004. The approximate region shown by the MODIS image is indicated by the thick black line in the CO tracer plot, and the green line indicates the position of the vertical section shown in Figure 8. MODIS fire detections are shown as black and red dots in the left and right images, respectively. Detections are for the entire day on the left plot but only for the respective MODIS Terra image in the right plot. Large black dots in the left image indicate the locations of Barrow on the far left and Alert in the top right corner. Note the strong distortion of the MODIS image, especially at the far left and right.

Figure 7: Transport episode in 2004.

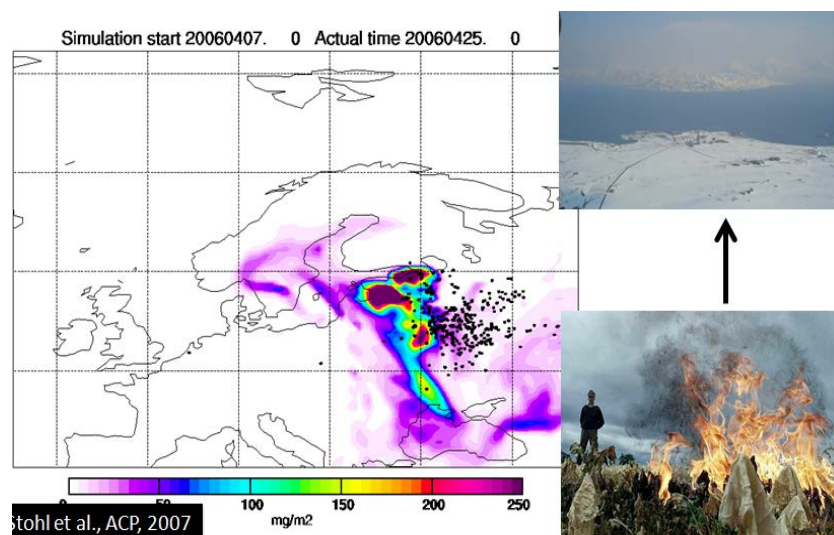


Figure 8: Transport episode in 2006.

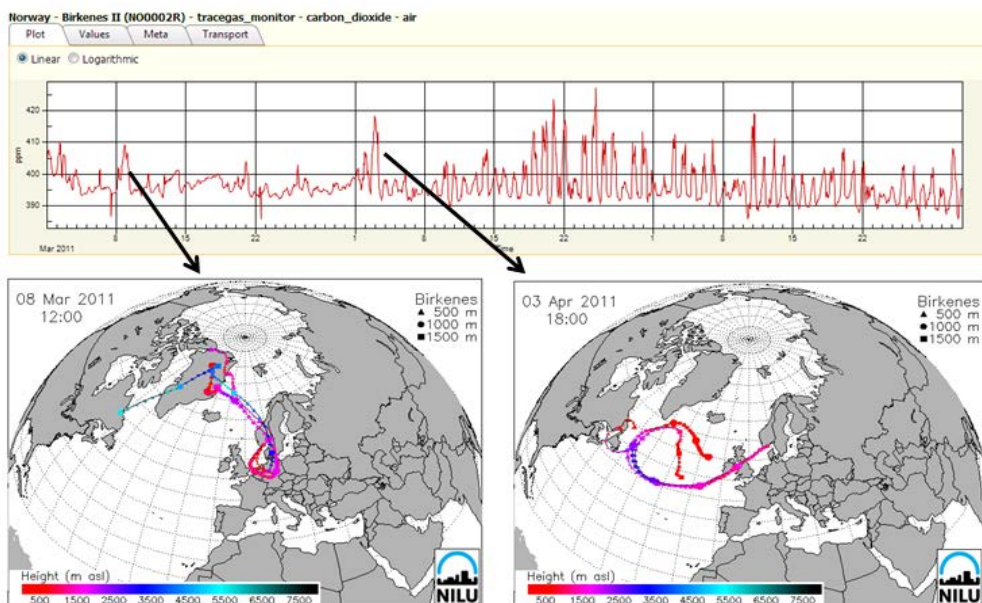


Figure 9: The CO₂ data from Birkenes in Mars-May 2011. The two selected episodes (8.March and 3.April 2011) both have enhanced values in the CO₂ mixing ratio measured at Birkenes. From the trajectories we find that the air masses come from the south and south-west on these two days, respectively.

Trajectory statistics performed for Birkenes 2011 shows that 85% of the trajectories in the time period Mar-May 2011 are arriving from the west. The number for Mar-May 2010 is 78%.

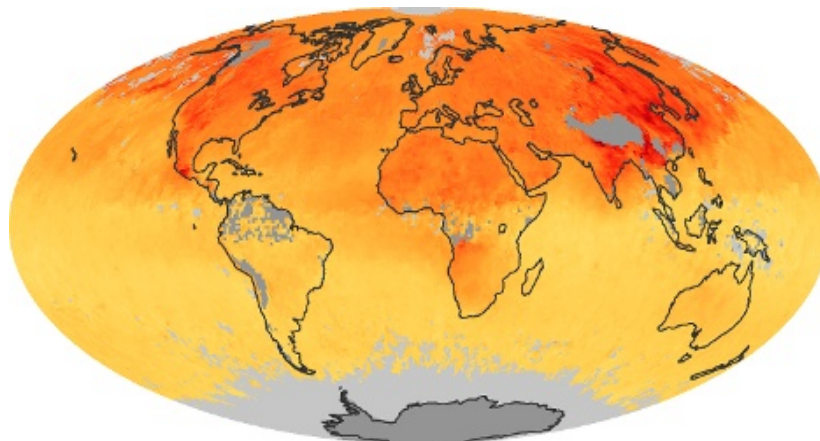


Figure 10: Monthly average CO 12.000 ft, MOPITT.

Figure 10 shows the monthly average of CO as measured by the MOIPTT instrument onboard the Terra satellite. One aim in the future is to investigate if other CO products from EO-platforms are more suitable for our purposes.

The results of the analysis were included in the KLIF report “*Monitoring of greenhouse gases and aerosols at Svalbard and Birkenes: Annual report 2012*”, prepared for KLIF in 2012 (for full report see Myhre et al., 2012), see Appendix C.

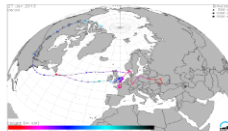
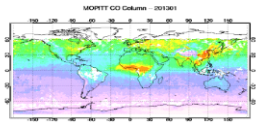
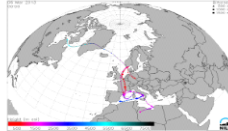
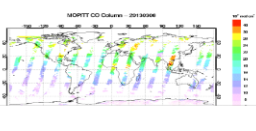
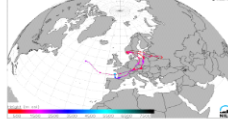
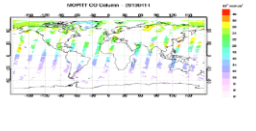
Preparing for operational use:

Based on the work and methodology developed in SatMoNAir and described above we have prepared a small portfolio of tools for detection and classification of high aerosol episodes in the spring of 2013. By using the EO overpass data from MODIS and the FIRMS products in combination with an e-mail alert system for warnings of when the NRT in-situ data from Zeppelin and Birkenes exceed certain pre-defined limit concentrations, we aim to be more prepared for e.g. providing rapid delivery information to other scientist and for reporting to the authorities.

The system is in operation and we have been using the products from FIRMS to investigate a number of fire “hotspots” in the Eastern Europe and Russian areas during spring time 2013, as these are relevant regions for long-range transport of aerosols to Norway and Scandinavia.

The developed alert system is in operation. Table 2 below shows a summary of events detected during early 2013, until 15.04.2013. The Warning level of CO₂ was set to 403 ppm, but this is still under testing and evaluation to find the most appropriate value.

Table 2: Events detected early 2013.

Date	FLEXTRA Traj. plot	FIRMS Fire (accumulated over 6 days prior to the high CO ₂ measurement)	Satellite CO ₂ *, monthly and daily plots
27.01.2013: Measured NRT CO ₂ : 419 ppm			
06.03.2013 Measured NRT CO ₂ : 408 ppm			
14.04.2013: Measured NRT CO ₂ : 410 ppm			

* http://www.acd.ucar.edu/mopitt/MOPITT/data/plots5j/maps_mon.html

1.4 References

- Di Pierro, M., Jaeglé, L., Eloranta, E. W., and Sharma, S.: Spatial and seasonal distribution of Arctic aerosols observed by the CALIOP satellite instrument (2006–2012), *Atmos. Chem. Phys.*, 13, 7075–7095, doi:10.5194/acp-13-7075-2013, 2013.
- Glantz, P. M. Tesche, H. Struthers, and K. Stebel, Satellite and ground-based observations of aerosol optical properties in the Arctic for the period 2003–2011, poster presented at the CRAICC meeting, Oslo, 26th – 28th August, 2012.
- Glantz, P., Johansson, C., Kokhanovsky, A., and von Hoyningen-Huene, W. (2009): Estimating PM_{2.5} over southern Sweden using space- borne optical measurements, *Atmos. Environ.*, 43, 5838–5846.
- Istomina, L.G., W. von Hoyningen-Huene, A.A. Kokhanovsky, and J.P. Burrows (2009), Retrieval of aerosol optical thickness in arctic region using dual-view AATSR observations, Proceedings of ESA Atmospheric Science Conference, Barcelona, 07.-11. Sept.2009. ESA SP-676.
- Istomina, L. G., von Hoyningen-Huene, W., Kokhanovsky, A. A., Schultz, E., and Burrows, J. P. (2011): Remote sensing of aerosols over snow using infrared AATSR observations, *Atmos. Meas. Tech.*, 4, 1133–1145, doi:10.5194/amt-4-1133-2011.
- Kristiansen, N. I., A. Stohl, A. J. Prata, A. Richter, S. Eckhardt, P. Seibert, A. Hoffmann, C. Ritter, L. Bitar, T. J. Duck, and K. Stebel, (2010), Remote sensing and inverse transport modeling of the Kasatochi eruption sulfur dioxide cloud, *J. Geophys. Res.*, 115, D00L16, doi:10.1029/2009JD013286.
- Mei, L., Y. Xue, G. de Leeuw, W. von Hoyningen-Huene, A. A. Kokhanovsky, L. Istomina, and J. Guang, J. P. Burrows (2013), Aerosol optical depth retrieval in the Arctic region using MODIS data over snow, *Remote Sensing of Environment*, 128, 21 January 2013, Pages 234–245, ISSN 0034-4257, <http://dx.doi.org/10.1016/j.rse.2012.10.009>.
- Myhre, C.L, Toledano, C., Myhre, G., Stebel, K., Yttri, K. E., Aaltonen, V., Johnsrud, M., Frioud, M., Cachorro, V., de Frutos, A., Lihavainen, H., Campbell, J. R., Chaikovskiy, A. P., Shiobara, M., Welton, E. J., and Tørseth, K., (2007) Regional aerosol optical properties and radiative impact of the extreme smoke event in the European Arctic in spring 2006, *Atmos. Chem. Phys.*, 7, 5899–5915, doi:10.5194/acp-7-5899-2007.
- Myhre, C.L., Hermansen, O., Fjæraa, A.M., Lunder, C., Fiebig, M., Schmidbauer, N., Krognæs, T., Stebel, K. (2012) Monitoring of greenhouse gases and aerosols at Svalbard and Birkenes: Annual report 2010. Kjeller, NILU (Statlig program for forurensningsovervåking. Rapport 1117/2012. TA-2902/2012) (NILU OR, 14/2012).
- Myhre, G., Stordal, F., Johnsrud, M., Diner, D. J., Geogdzhayev, I. V., Haywood, J. M., Holben, B. N., Holzer-Popp, T., Ignatov, A., Kahn, R. A., Kaufman, Y. J., Loeb, N., Martonchik, J. V., Mishchenko, M. I., Nalli, N. R., Remer, L. A., Schroedter-Homscheidt, M., Tanré, D., Torres, O., and Wang, M.: Intercomparison of satellite retrieved aerosol optical depth over ocean during the period September 1997 to December 2000, *Atmos. Chem. Phys.*, 5, 1697–1719, doi:10.5194/acp-5-1697-2005, 2005.
- Schaap, M. R.M.A. Timmermans , R.B.A. Koelemeijer, G. de Leeuw, P.J.H. Builtjes, Evaluation of MODIS aerosol optical thickness over Europe using sun photometer

observations, *Atmos. Environ.*, 42, 2187–2197, doi:10.1016/j.atmosenv.2007.11.044, 2008.

Sodemann, H., Pommier, M., Arnold, S. R., Monks, S. A., Stebel, K., Burkhardt, J. F., Hair, J. W., Diskin, G. S., Clerbaux, C., Coheur, P.-F., Hurtmans, D., Schlager, H., Blechschmidt, A.-M., Kristjánsson, J. E., and Stohl, A. (2011): Episodes of cross-polar transport in the Arctic troposphere during July 2008 as seen from models, satellite, and aircraft observations, *Atmos. Chem. Phys.*, 11, 3631-3651, doi:10.5194/acp-11-3631-2011.

Stohl, A., T. Berg, J. F. Burkhardt, A. M. Fjæraa, C. Forster, A. Herber, Ø. Hov, C. Lunder, W.W. McMillan, S. Oltmans, M. Shiobara, D. Simpson, S. Solberg, K. Stebel, J. Ström, K. Tørseth, R. Treffeisen, K. Virkkunen, and K. E. Yttri (2006): Pan-Arctic enhancements of light absorbing aerosol concentrations due to North American boreal forest fires during summer 2004. *J. Geophys. Res.* 111 , D22214, doi:10.1029/2006JD007216.

Stohl, A., Berg, T., Burkhardt, J. F., Fjæraa, A. M., Forster, C., Herber, A., Hov, Ø., Lunder, C., McMillan, W. W., Oltmans, S., Shiobara, M., Simpson, D., Solberg, S., Stebel, K., Ström, J., Tørseth, K., Treffeisen, R., Virkkunen, K., and Yttri, K. E. (2007): Arctic smoke - record high air pollution levels in the European Arctic due to agricultural fires in Eastern Europe. *Atmos. Chem. Phys.* 7, 511-534 .

Toledano, C. V.E. Cachorro, M. Gausa, K. Stebel, V. Aaltonen, A. Berjón, J.P. Ortiz de Galisteo, A.M. de Frutos, Y. Bennouna , S. Blindheim, C.L. Myhre, G. Zibordi, C. Wehrli, S. Kratzer, B. Hakansson, T. Carlund, G. de Leeuw, A. Herber, and B. Torres, (2012), Overview of sun photometer measurements of aerosol properties in Scandinavia and Svalbard, *Atmospheric Environment* 52, 18-28.

von Hardenberg, J., Vozella, L., Tomasi, C., Vitale, V., Lupi, A., Mazzola, M., van Noije, T. P. C., Strunk, A., and Provenzale, A. (2012): Aerosol optical depth over the Arctic: a comparison of ECHAM-HAM and TM5 with ground-based, satellite and reanalysis data, *Atmos. Chem. Phys.*, 12, 6953-6967, doi:10.5194/acp-12-6953-2012.

Winker, D. M., Tackett, J. L., Getzewich, B. J., Liu, Z., Vaughan, M. A., and Rogers, R. R. (2013): The global 3-D distribution of tropospheric aerosols as characterized by CALIOP, *Atmos. Chem. Phys.*, 13, 3345-3361, doi:10.5194/acp-13-3345-2013.

2 Use of satellite based ozone measurements in national reporting (WP 2)

2.1 Monitoring of the atmospheric O₃ layer and UV radiation

The work in WP 2 includes analyses of satellite data to support ground based ozone measurements in the Norwegian national monitoring programme 'Monitoring of the atmospheric ozone layer and natural ultraviolet radiation'.

It is important to follow the development of the ozone layer in order to verify that the Montreal Protocol and its amendments work as expected and detect other possible changes in the ozone layer. KLIF established the programme "Monitoring of the atmospheric ozone layer" in 1990 and NILU has been responsible for the operation and maintenance of the monitoring programme since the start. Currently the program includes measurement of total ozone (the ozone layer) and UV at three locations (Oslo, Andøya and Ny-Ålesund). The purpose of the programme is to:

- Provide continuous measurements of total ozone and natural ultraviolet radiation that reach the earth surface
- Provide data that can be used for trend analysis of both total ozone and natural ultraviolet radiation.
- Provide information on the status and the development of the ozone layer and natural ultraviolet radiation
- Notify the Climate and Pollution Agency when low ozone/high UV episodes occur.

There are four tasks under WP 2, which are described in the following

2.2 Satellite ozone measurements

Methodologies for spatial data analysis

The work has focused on data analysis and development of tools for making assessments of the mapping capability of the satellites. This includes correlation, mean and standard deviation between satellite products, and comparisons to ground based measurements. Available satellite products have been re-gridded to 1x1 degree resolution and both daily and monthly mean gridded ozone data have been studied globally and regionally (an extended Scandinavian region). Some satellites, e.g. SCIAMACHY, is not optimal for gridded monthly mean comparisons since the spatial coverage is relatively poor and the monthly mean values are calculated from relatively few observations. Figure 11 (upper) shows the difference between SCIAMACHY and OMI on an arbitrary day, whereas Figure 11 (lower) shows the monthly mean comparison between the two satellites. The characteristic stripes are caused by the lack of SCIAMACHY overpass data, which also results in misleading estimates of monthly standard deviation between the satellites.

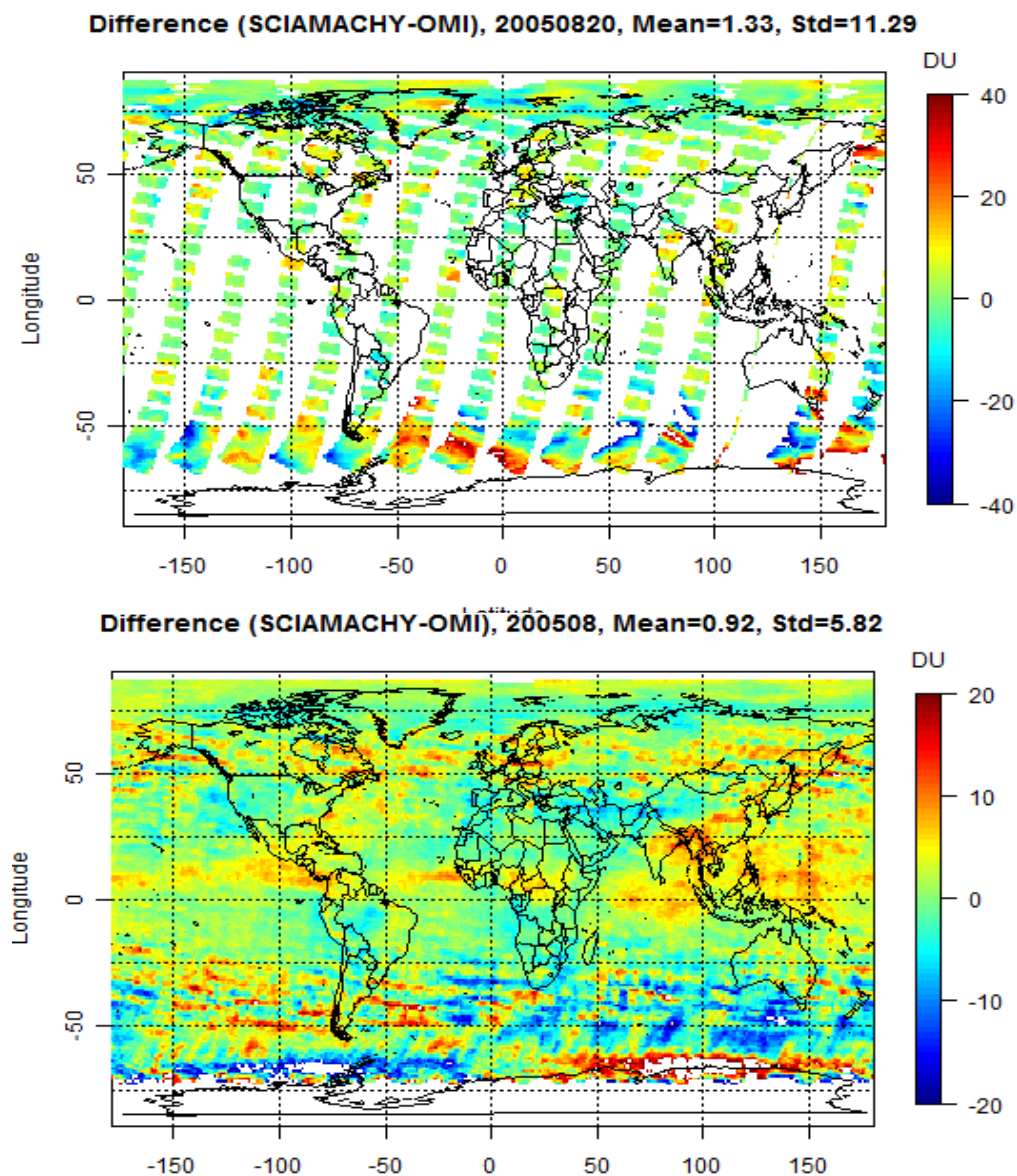


Figure 11: Daily ozone (upper panel) and monthly mean ozone (lower panel) difference between SCIAMACHY and OMI an arbitrary day and month.

In general the difference-plots give a good indication of the temporal and spatial behaviour of the satellites over selected regions. A full assessment of the satellites is not carried out, but the tools and methodology are made available through this project.

2.3 Satellite based time-series of ozone

The work on satellite based time-series at selected locations (Oslo, Andøya and Ny-Ålesund) and comparisons to ground based measurements, was more or less finished during the first phase of SatMoNAir.

Our recent work has focused on global and regional ozone trend analyses from satellites. These trend studies are based on daily and monthly gridded ozone data from 1978 until present. Ground based ozone measurements from Oslo have previously revealed a significant negative trend from 1978 until mid 1990s, especially during winter and spring, whereas no significant trend is observed for the last two decades. It is of great interest to compare ground based and satellite retrieved ozone trends and also study latitudinal and longitudinal variations. New R programs have been designed to make gridded linear regression analyses and trend estimates. Figure 12 shows results from this study. The 1978-2011 EO ozone time series is divided into two periods: 1) 1979-1993, which is entirely based on TOMS (Nimbus7) data, and 2) the period from 1996 to present. For the latter time period different combinations of satellite products can be selected. Because ozone trends might be strongly seasonal dependent, trends are calculated for all 12 months separately. Figure 12 shows trends from April: Left panel represent the period 1978-1993, whereas the right panel represent the period 1996-2011. The latter trend calculations are based on TOMS (EarthProbe) data from 1996-2004 and OMI data from 2005 and onward.

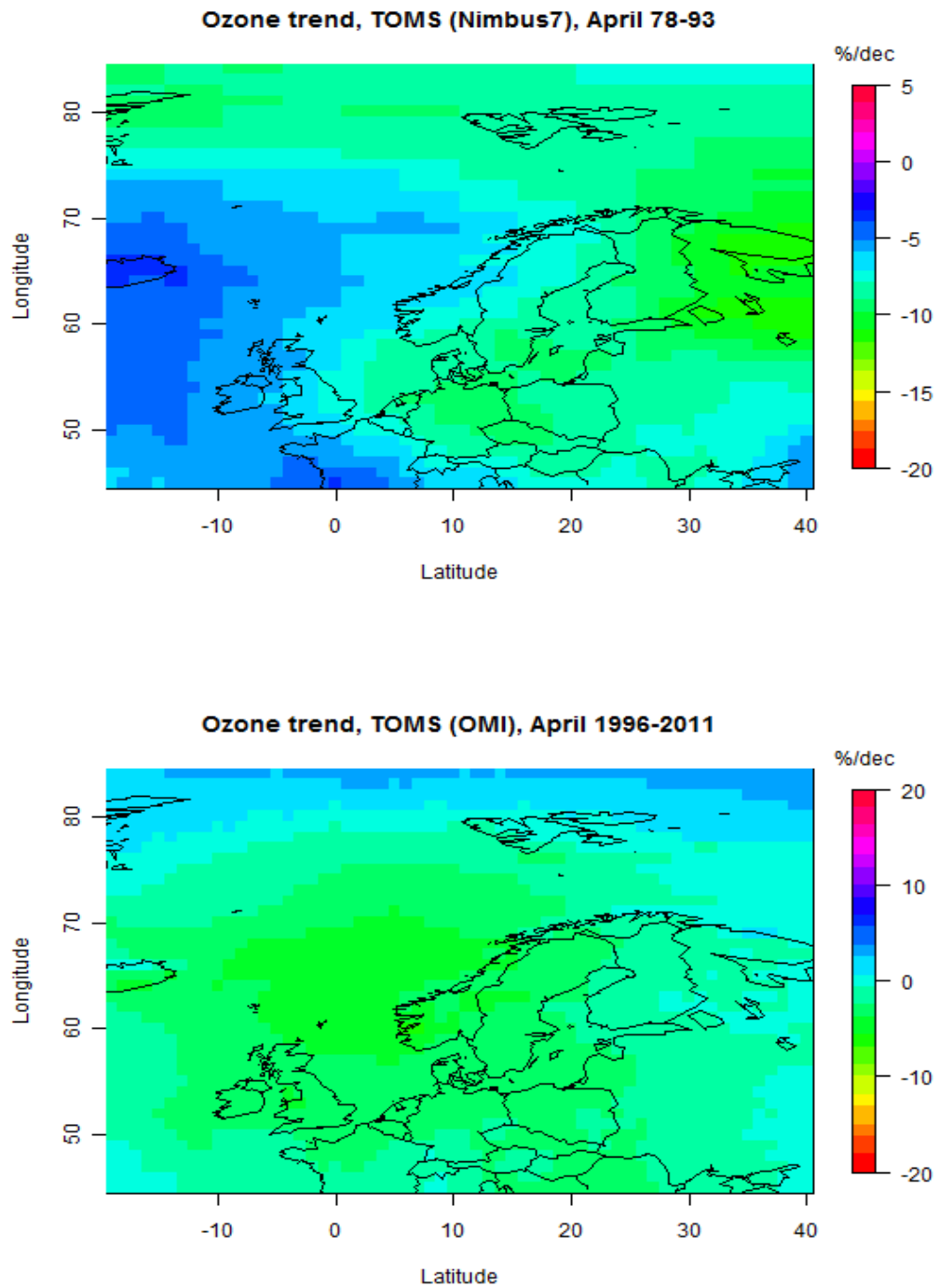


Figure 12: April ozone trend from 1978-1993 (upper panel) and 1996-2011 (lower panel) retrieved from TOMS and OMI satellites. Note that the scale is different in the two plots.

The trend analyses can also be extended to larger regions. Figure 13 shows a global map of October ozone trend for the period 1978-1993, where the Antarctic ozone hole can be clearly seen. Over Antarctica the negative ozone trend was as large as 35-40%/decade during these years.

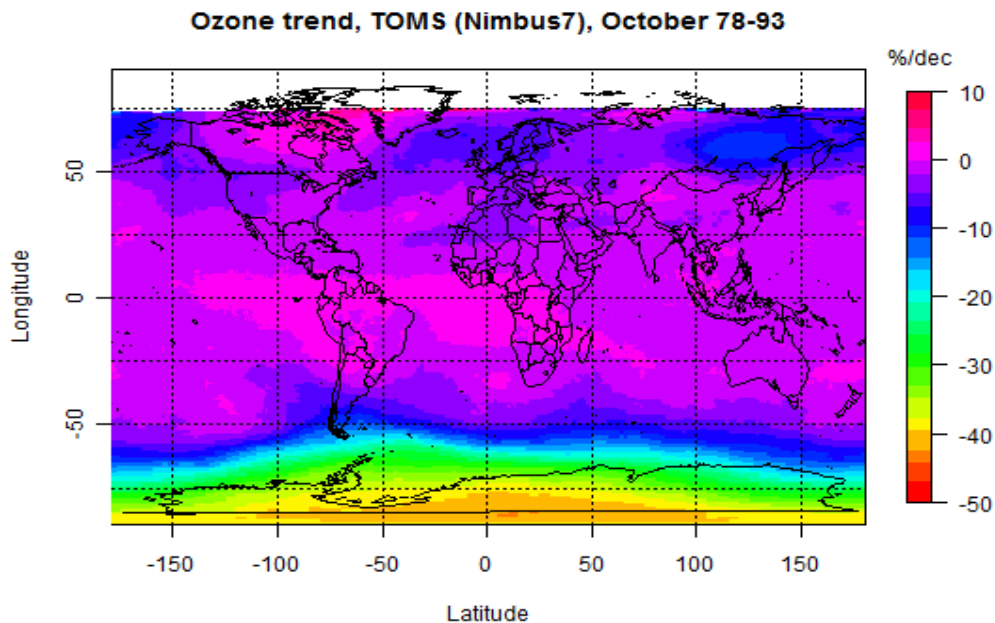


Figure 13: Global October ozone trend for the period 1978-1993. The analyses are based on TOMS Nimbus 7 data.

2.4 Analysis and reporting

The annual KLIF report in 2012 on “Monitoring of the atmospheric ozone layer and natural ultraviolet radiation” (Svendby et al., 2012) had a separate chapter on ‘Satellite observations of ozone above Norway and the Norwegian Arctic region’, which is given as Appendix D. This work was directly linked to the current WP of the SatMoNAir project. The 2013 KLIF report will include additional SatMoNAir work, particularly the recent work on trend studies.

2.5 References

- Svendby, T.M., Myhre, C.L., Stebel, K., Edvardsen, K., Orsolini, Y., Dahlback, A. (2012) Monitoring of the atmospheric ozone layer and natural ultraviolet radiation. Annual report 2011. Kjeller, NILU (Statlig program for forensningsovervåking. Rapport 1129/2012. TA-2952/2012) (NILU OR, 29/2012).

3 Satellite based Air Quality monitoring of remote areas for EMEP reporting (WP 3)

3.1 Introduction

The main objective of the EMEP program (Co-operative Programme for Monitoring and Evaluation of the Long-Range Transport of Air Pollutants in Europe) consists of the regular provision of qualified scientific information to governments and subsidiary bodies and to evaluate the international protocols on emission reductions that have been negotiated within the Convention on Long Range Transboundary Air Pollution (LRTAP).

The EMEP monitoring programme, which is being coordinated by the EMEP Chemical Coordinating Centre (EMEP-CCC) hosted by the Norwegian Institute for Air Research (NILU), currently consists of 100 European stations measuring a wide variety of atmospheric pollutants. The EMEP monitoring strategy is traditionally based on measurements at ground stations, however since the station density in Eastern Europe is particularly low and thus cannot provide much spatial information, it is highly desirable to evaluate the suitability of satellite observations of atmospheric composition to complement the in situ measurements carried out today.

Satellite remote sensing can be valuable source of information for a wide variety of fields including the atmosphere. Operational satellite remote sensing of NO₂ and other atmospheric constituents has been carried out since 1995 when the Global Ozone Monitoring Experiment (GOME) (Burrows et al., 1999; Richter and Burrows, 2002) was first launched. Beginning in 2002, the observations were continued by the SCIAMACHY (SCanning Imaging Absorption spectroMeter for Atmospheric CartographY) sensor onboard of Envisat (Bovensmann et al., 1999; Gottwald et al., 2006), and subsequently complemented in 2004 by the Ozone Monitoring Instrument (OMI) (Levelt et al., 2006) as well as the Global Ozone Monitoring Experiment-2 (GOME-2) instrument in 2006 (Munro et al., 2006).

3.2 Methodology

The EECCA region

The Eastern Europe, Caucasus and Central Asia (EECCA) region is a group of countries in Eastern Europe and Asia. It includes Armenia, Azerbaijan, Belarus, Georgia, Kazakhstan, Kyrgyzstan, Moldova, the Russian Federation, Tajikistan, Turkmenistan, Ukraine and Uzbekistan. Figure 1 provides a map of the entire study area.



Figure 14: Map of the EECCA region (Eastern Europe, Caucasus and Central Asia)

Satellite data

Satellite data from four different instruments was acquired and used for this study: These are GOME, SCIAMACHY, OMI, and GOME-2 and are described in the following sections.

a. GOME

Launched in 1995 onboard of the 2nd European Remote Sensing Satellite (ERS-2), the Global Ozone Monitoring Experiment (GOME) was one of the first spaceborne instruments primarily targeted towards analysing the composition of the atmosphere (Burrows et al., 1999). The instrument is a grating pseudo double monochromator which covers the spectral range of 240 nm to 790 nm at a spectral resolution of 0.2 nm to 0.4 nm (Richter and Burrows, 2002).

GOME has been used for a wide variety of applications, in particular for the operational production of global products of ozone and NO₂ (Richter and Burrows, 2002). Research products were also developed for some minor trace gases such as OCIO, volcanic SO₂, H₂CO, and tropospheric BrO. The spatial resolution of a GOME ground pixel is 40 x 320 km². The overpass time of GOME is approximately 10:20 local time.

b. SCIAMACHY

SCIAMACHY (SCanning Imaging Absorption spectroMeter for Atmospheric Cartography) is a hyperspectral UV/VIS/NIR passive imaging grating spectrometer observing the wavelength range of 214--2386 nm (Bovensmann et al., 1999; Gottwald et al., 2006). Its overpass time is approximately 10:00 local time at the equator. The data acquired by the instrument has been used for a wide variety of operational and research applications Gottwald et al. (2006). Monthly averaged SCIAMACHY NO₂ data were obtained from the Tropospheric Emission Monitoring Internet Service (TEMIS) website and from the website of the Institute of Environmental Physics (IUP) of the University of Bremen.

c. OMI

The Ozone Monitoring Instrument (OMI) is based on the experiences acquired from both GOME and SCIAMACHY. It combines their advantages, measuring the complete spectrum in the UV/VIS wavelength range at a comparatively high spatial resolution of 13 km x 24 km, while providing daily global coverage.

The OMI instrument is flying on the National Aeronautics and Space Administration's Earth Observing System Aura platform as part of the A-train constellation of satellites. In contrast to all the other instruments mentioned here, which have equator crossing times around 10:00 local time, OMI has an equator crossing time of approximately 1:45 LST in the afternoon, and therefore probes the Earth's atmosphere under different conditions. Aura/OMI was launched in 2004 and has been continuously providing data. Beginning in June 2007, OMI has suffered from several row anomalies affecting the quality of the Level 1B and Level 2 data products. Level-3 products are produced after filtering for the affected anomalies.

d. GOME-2

The Global Ozone Monitoring Experiment-2 (GOME-2) is a scanning spectrometer onboard of the MetOp series of satellites. As a modified and improved successor of ERS-2's GOME instrument, GOME-2 measures in a spectral range of 240 nm to 790 nm with a varying spectral resolution between 0.24 nm and 0.53 nm (Callies et al., 2000). The spatial resolution of the instrument is 40 km x 40 km. For this project, monthly GOME-2 NO₂ data was acquired from www.temis.nl. The product was generated using the standard TEMIS algorithm (Boersma et al., 2011).

TEMIS NO₂ Retrieval Algorithm

In short, the TEMIS NO₂ retrieval is based on three steps: The first step of the algorithm consists of a Differential Optical Absorption Spectroscopy (DOAS) retrieval of the total slant column of NO₂ from the measured spectrum, where absorption cross sections of NO₂, ozone, H₂O as well as a synthetic ring spectrum are taken into account, and a fifth order polynomial is included in the fit to account for scattering effects.

The second step consists of the separation of the stratospheric and tropospheric NO₂ contributions to the total NO₂ column, where the stratospheric NO₂ column is estimated by assimilating total slant columns in the TM4 chemistry transport model (Dentener et al., 2003; Boersma et al., 2007). The third and final step of the retrieval is the conversion of the tropospheric NO₂ slant columns into vertical columns using a calculated Air-Mass Factor (AMF). Further details on the specific retrieval methodology can be found in Boersma et al. (2004), Boersma et al. (2007), and Boersma et al. (2011), as well as on the TEMIS website (www.temis.nl). Solely data reprocessed with version 2.0 of the retrieval algorithm was used. Improvements in version 2.0 over previous versions of the retrieval algorithm include an updated albedo database, a modified calculation of the air mass factor, a correction of the surface height calculation, a correction of

the weekly cycle in NO_x emissions, as well as an increased number of NO_x tracers in the applied chemical transport model (Boersma et al., 2011). The NO₂ data set used here only considered cloud radiance fractions of less than 50%. It was also re-sampled from the original SCIAMACHY spatial resolution to a 0.25 x 0.25 degree grid. For this study, monthly data between August 2002 and August 2011 was available.

Although the NO₂ dataset used in this study is based to some extent on data assimilation using the TM4 model (Dentener et al., 2003; Boersma et al., 2007), it is almost independent of the used emission inventory due to the retrieval set-up. The data assimilation results are mainly used to provide the stratospheric NO₂ column in the second step. This stratospheric column is virtually independent of the used emission database. For the calculation of the AMF in the third step knowledge of the profile shape of the vertical NO₂ distribution is needed. This profile shape is also taken from the data assimilation. However, the profile shape is independent of the emissions, since the data assimilation is scaling the NO₂ column with conservation of the shape. In conclusion, the NO₂ data are considered as retrieval results independent of emission data.

Ground data

In situ data was obtained from air quality stations within the EMEP network. The data was acquired from the EBAS database (ebas.nilu.no), which is operated by NILU.

Figure 14 shows the spatial distribution of all stations within the EECCA region for which the EMEP network provides data of NO₂ and SO₂. Note that all stations are located in the very western extent of the EECCA region, while the entire rest of the region exhibits a complete lack of any in situ data. Four of the stations are located in Russia, one station in Moldova, another station in Georgia, and one station is situated in Armenia.

Five stations provided NO₂ measurements at some point between 1995 and 2012, however none of them provided a continuous data record. The stations also only provided daily averages and not hourly observations. Seven stations throughout the EECCA region provided observations of SO₂ for the study period between 1995 and 2012. These are identical to the stations providing NO₂ data with the addition of RU0018R and GEO0001R.

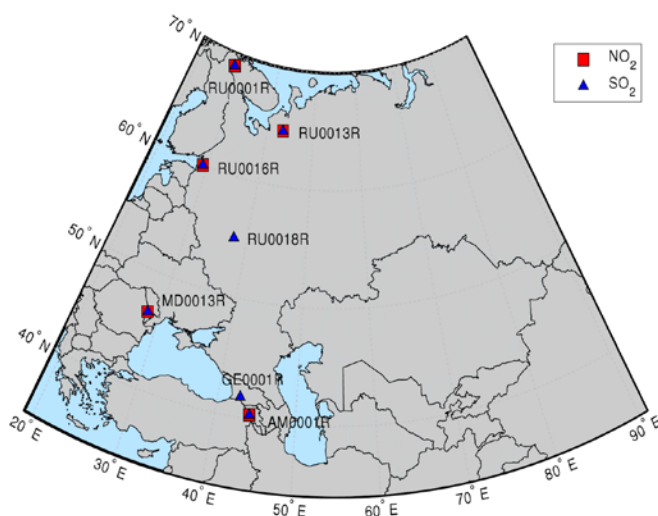


Figure 15: Overview of the spatial distribution of suitable EMEP stations

3.3 Results

Tool development

A variety of tools have been implemented within the framework of this project in the Matlab programming environment. This includes code for purposes of data acquisition, data import/reading, re-gridding and processing, data extraction, and data analysis for a total of four different satellite instruments (GOME, SCIAMACHY, OMI, GOME-2).

The major tools developed were:

1. Automated downloading of datasets from various servers
2. Reading the different data formats (ASCII, HDF)
3. Batch processing of entire directories of monthly/daily files to generate "data stacks" from which to compute time series
4. Extracting time series of NO₂ and SO₂ at any point on the globe. This can be done over single grid cells or as the average over a specified grid cell array. For NO₂ this produces times series from 1995 to 2012, for SO₂ from 2002 to 2012
5. Masking images using the outline of the EECCA study region
6. Differencing images as part of the product inter-comparison exercises
7. Computing country averages and country-level statistics
8. Map production and visualization

In addition to these major tools, a wide variety of minor code development was performed. This task also included the acquisition of various complete data sets of monthly and daily satellite data from the various sensors.

3.3.1 Long-term average Mapping

NO₂

Maps of long-term average concentrations are very helpful for studying consistent spatial patterns in concentrations as they reduce the noise in the data. Figure 16 shows the long-term mean concentration of tropospheric NO₂ over the EECCA region, calculated between August 2002 and March 2012.

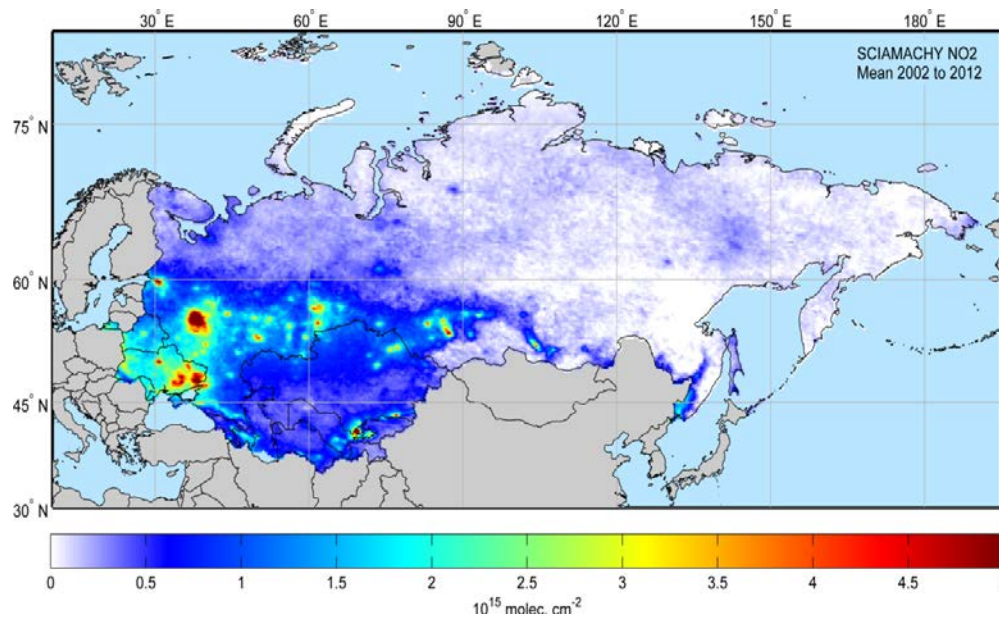


Figure 16: Long-term average tropospheric NO₂ concentration derived from SCIAMACHY between August 2002 and March 2012.

SO₂

In general, the operational space-borne SO₂ products are intended for detection of very strong SO₂ emission events such as volcanic eruptions. While it is possible to detect some anthropogenic sources of SO₂, only the very strongest of such signals will be distinguishable from the background noise. Examples are shown in Figure 17 and Figure 18 which indicate the long-term average SO₂ concentrations over the EECCA region generated from SCIAMACHY and OMI data, respectively. Both products suffer from negative values in some areas, however OMI is able to provide slightly more spatial detail. Figure 19 shows the difference image between the two products.

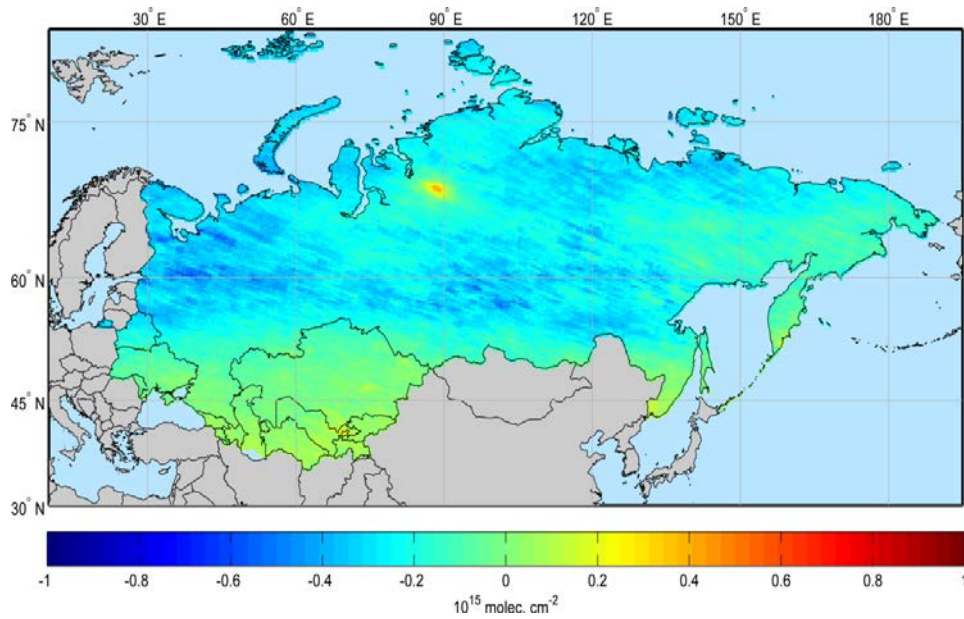


Figure 17: Long-term average SO_2 concentration derived from SCIAMACHY-TEMIS between January 2004 and March 2012. Note that the values can become negative due the retrieval algorithm's tendency to be affected by interference from ozone.

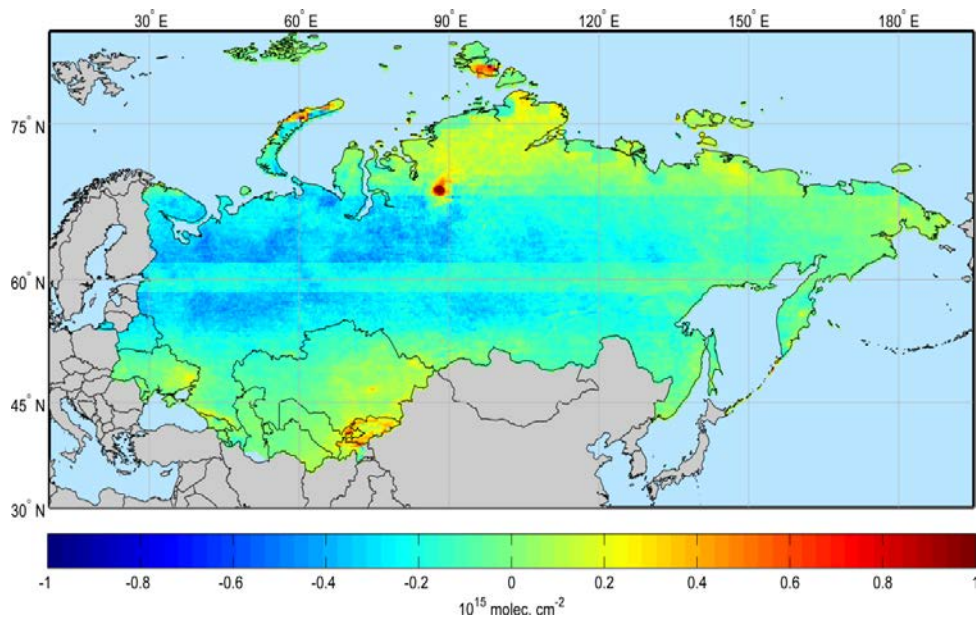


Figure 18: Long-term average SO_2 concentration derived from OMI between January 2005 and December 2011. Note that the values can become negative due the retrieval algorithm's tendency to be affected by interference from ozone.

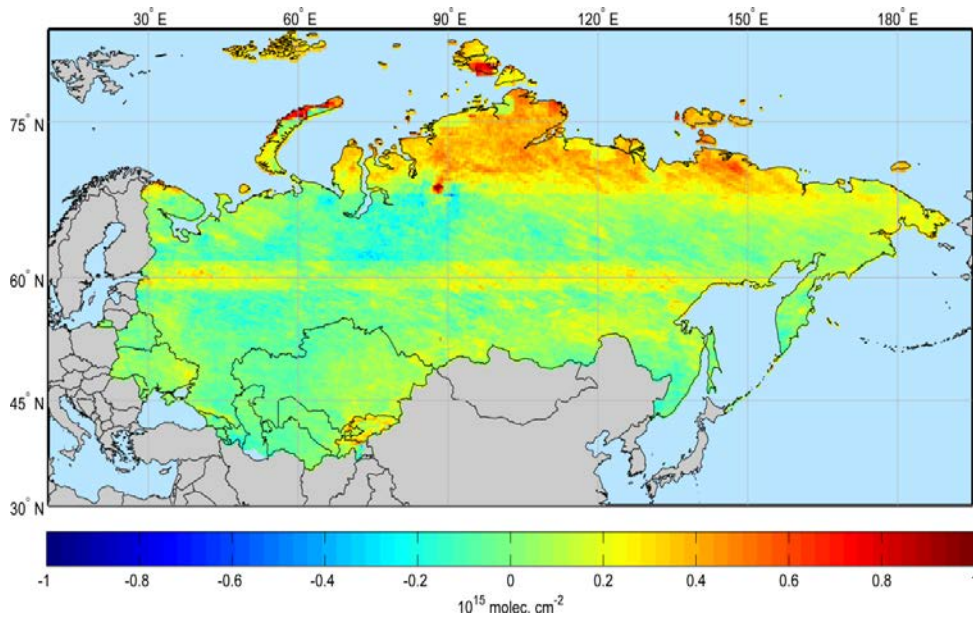


Figure 19: Difference image calculated from the long-term averages as OMI-NASA minus SCIAMACHY-SACS.

3.3.2 Product inter-comparison

Figure 20 through Figure 23 provide long-term average difference images of the various combinations of NO_2 products over the EECCA region.

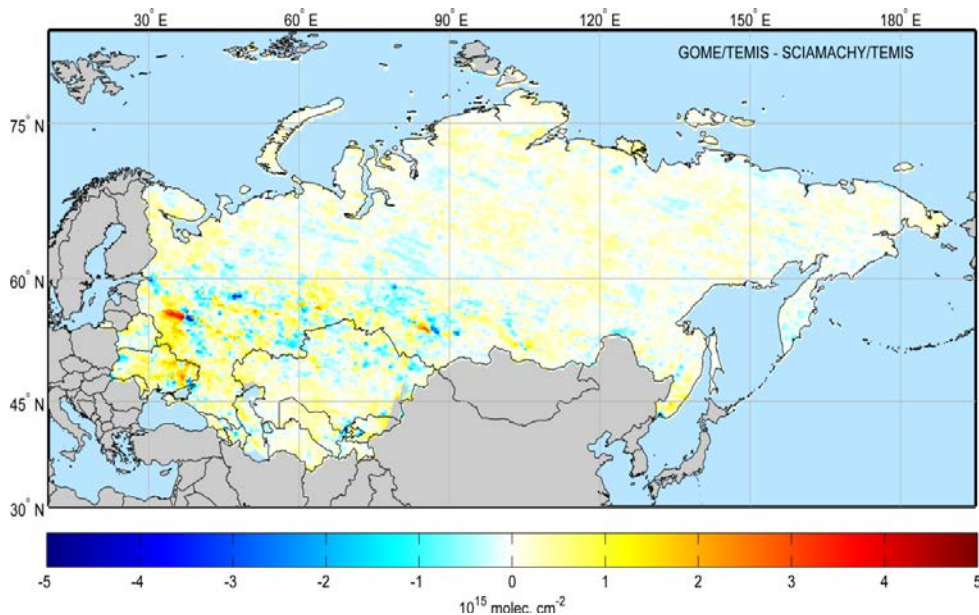


Figure 20: Difference image showing the absolute biases between the GOME/TEMIS and the SCIAMACHY/TEMIS products. It was computed over the entire overlap period between both products from August 2002 to June 2003. The bias was calculated as GOME/TEMIS minus SCIAMACHY/TEMIS.

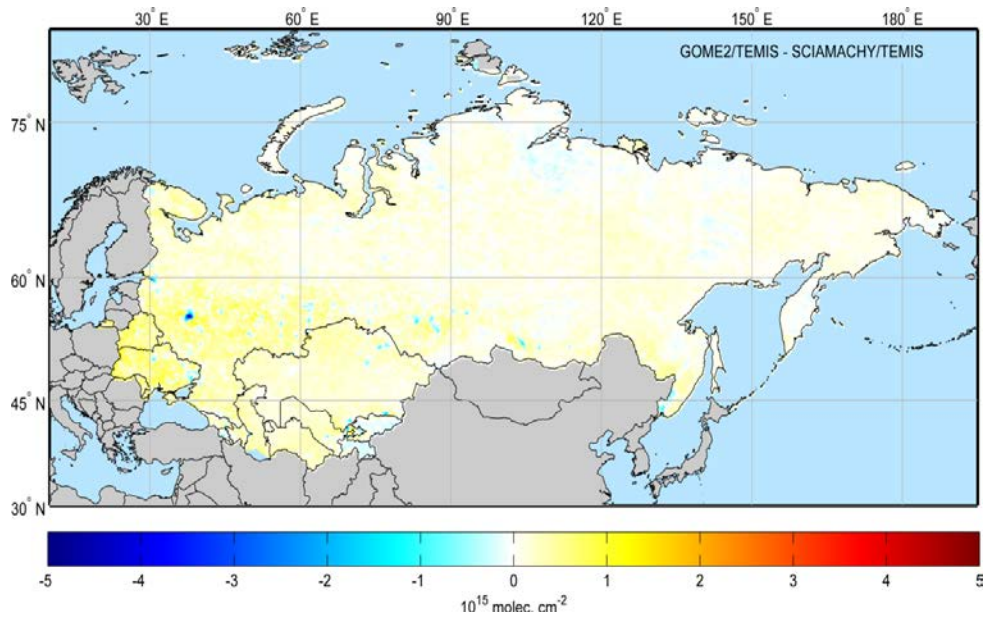


Figure 21: Difference image showing the absolute biases between the GOME2/TEMIS and the SCIAMACHY/TEMIS products. It was computed over the entire overlap period between both products from January 2007 to March 2012. The bias was calculated as GOME2/TEMIS minus SCIAMACHY/TEMIS.

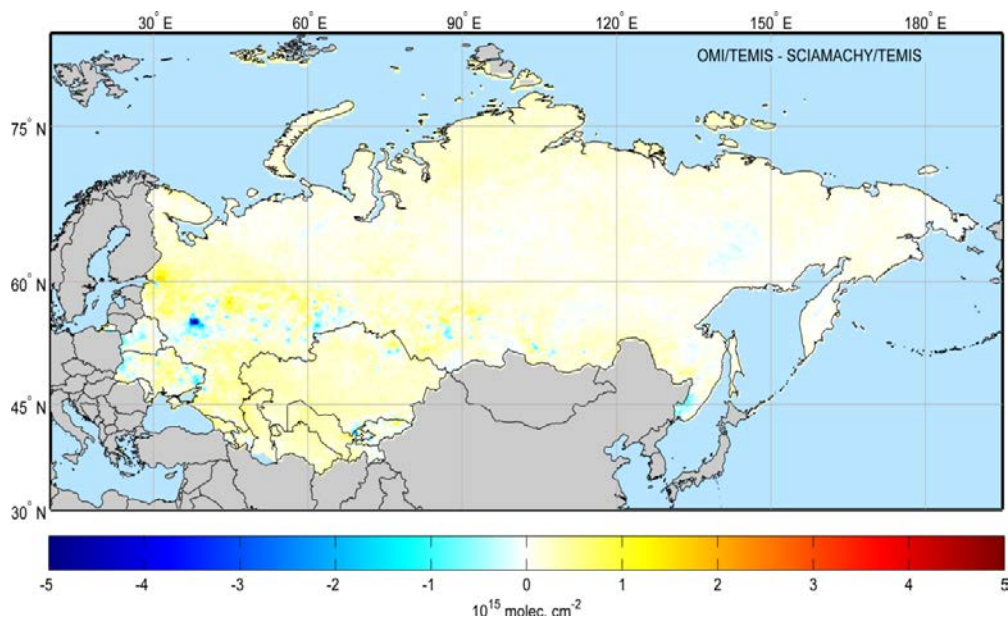


Figure 22: Difference image showing the absolute biases between the OMI/TEMIS and the SCIAMACHY/TEMIS products. It was computed over the entire overlap period between both products from October 2004 to March 2012. The bias was calculated as OMI/TEMIS minus SCIAMACHY/TEMIS.

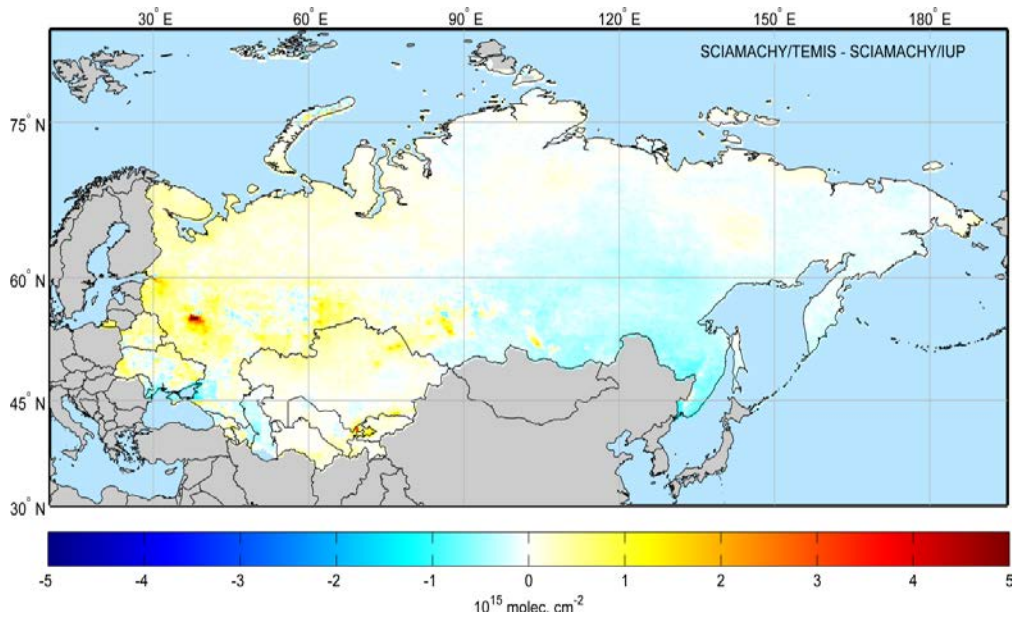


Figure 23: Difference image showing the absolute biases between the SCIAMACHY/TEMIS and the SCIAMACHY/IUP products. It was computed over the entire overlap period between both products from August 2002 to December 2011. The bias was calculated as SCIAMACHY/TEMIS minus SCIAMACHY/IUP.

While interpreting difference images of various products is quite valuable to determine spatial patterns in the corresponding biases, a quantitative comparison requires a statistical analysis. Here we compute country-level statistics from the difference images. Table 3 through Table 5 show country-level differences computed from various monthly NO₂ products

Table 3: Country-level difference statistics for the comparison of GOME-2/TEMIS product versus the SCIAMACHY/TEMIS product. Differences were computed as GOME-2 minus SCIAMACHY. The statistics were computed over the entire overlap period between both instruments from January 2007 to March 2012. All values given in units of 1015 molecules cm². MAE is the mean absolute error and RMSE denotes the root mean squared error.

Armenia	-0.020	0.195	0.195	0.128
Azerbaijan	0.154	0.194	0.247	0.203
Belarus	0.501	0.193	0.537	0.504
Georgia	0.117	0.200	0.231	0.187
Kazakhstan	0.179	0.141	0.228	0.195
Kyrgyzstan	-0.031	0.163	0.166	0.132
Moldova	0.414	0.164	0.445	0.414
Russia	0.117	0.162	0.200	0.141
Tajikistan	-0.058	0.200	0.207	0.157
Turkmenistan	0.223	0.101	0.245	0.228
Ukraine	0.421	0.294	0.514	0.459
Uzbekistan	0.165	0.214	0.270	0.212
Mean	0.182	0.185	0.290	0.247

Table 4: Country-level difference statistics for the comparison of GOME/TEMIS product versus the SCIAMACHY/TEMIS product. Differences were computed as GOME minus SCIAMACHY. The statistics were computed over the entire overlap period between both instruments from August 2002 to June 2003. All values given in units of 1015 molecules cm². MAE is the mean absolute error and RMSE denotes the root mean squared error.

Armenia	0.181	0.319	0.365	0.294
Azerbaijan	-0.022	0.451	0.451	0.327
Belarus	0.147	0.411	0.436	0.347
Georgia	0.047	0.344	0.346	0.274
Kazakhstan	0.084	0.398	0.407	0.294
Kyrgyzstan	0.209	0.407	0.457	0.345
Moldova	0.335	0.402	0.521	0.429
Russia	0.06	0.346	0.352	0.218
Tajikistan	0.039	0.27	0.273	0.19
Turkmenistan	0.108	0.207	0.233	0.184
Ukraine	0.422	0.728	0.841	0.66
Uzbekistan	0.096	0.5	0.509	0.301
Mean	0.142	0.399	0.432	0.322

Table 5: Country-level difference statistics for the comparison of OMI/TEMIS product versus the SCIAMACHY/TEMIS product. Differences were computed as OMI minus SCIAMACHY. The statistics were computed over the entire overlap period between both instruments from October 2004 to March 2012. All values given in units of 1015

molecules cm². MAE is the mean absolute error and RMSE denotes the root mean squared error.

Armenia	0.112	0.181	0.212	0.178
Azerbaijan	0.128	0.188	0.227	0.191
Belarus	-0.019	0.226	0.227	0.176
Georgia	0.266	0.207	0.337	0.295
Kazakhstan	0.217	0.155	0.267	0.237
Kyrgyzstan	0.058	0.216	0.224	0.158
Moldova	0.05	0.162	0.169	0.126
Russia	0.116	0.188	0.221	0.147
Tajikistan	0.075	0.197	0.21	0.156
Turkmenistan	0.252	0.106	0.273	0.256
Ukraine	0.116	0.297	0.319	0.254
Uzbekistan	0.261	0.255	0.364	0.308
Mean	0.136	0.198	0.254	0.207

With respect to Table 5 and in fact any product inter-comparison involving OMI data, it should be noted that in contrast to all the other satellite instruments used here (GOME, SCIAMACHY and GOME-2 with local overpass times between 9:30 and 10:30 LT), the OMI instrument onboard the Aura platform has a local overpass time in the early afternoon (approximately 13:45 LT). Given the often substantial daily cycle of NO₂, this roughly 4-hour difference in local overpass times can have a significant impact on the observed concentrations and thus on derived images and time series. Essentially, the difference in overpass times between OMI and the rest of the sensors means that the troposphere is sampled under different atmospheric conditions, which has a variety of implications (Richter et al., 2006):

1. Cloud cover is highly variable throughout the day and morning and afternoon can have significantly different cloud statistics depending on region. As NO₂ can only be retrieved during clear-sky conditions, this can therefore strongly affect the areas that are probed by instruments with different overpass times
2. The lightning activity over the continents generally tends to be at a minimum during the morning hours and increases towards the afternoon. As some of the tropospheric NO₂ detected by space-borne instruments, different overpass times can mean a different level of lightning-caused NO₂
3. The emission of NO_x are very much time-dependent due to local rush hours etc, and as a result there is often a strong diurnal cycle in emissions and therefore NO₂ columns
4. The daytime boundary layer evolves in the morning hours and is generally not fully developed during the time of the morning overpasses

Based on this work it is concluded that when using NO₂ data from multiple instruments, it is highly recommended to use a consistent algorithm throughout. At the moment, this can be most easily be accomplished by using data from www.temis.nl, which provides daily and monthly NO₂ products from all four major instruments derived with a consistent methodology.

An experimental 0.1 degree x 0.1 degree (about 10 km x 10 km) spatial resolution OMI NO₂ product was further acquired from NASA Goddard. The grid cell size of this product is closer to the original spatial resolution at which OMI measures tropospheric column (13 km x 24 km) than the grid used for the standard OMNO2e product (0.25 degree x 0.25 degree) and can thus better represent small-scale spatial variability. This can be seen in Figure 24, which shows a comparison of the two products for the Po valley region of Northern Italy. Small hotspots such as that over Torino in the very western part of the Po valley can be easily identified in the high-resolution product, whereas it shows only very weakly in the standard resolution product.

The existence of this experimental product is important as it gives an indication of what the TROPOMI instrument onboard the future Sentinel-3 satellite will be capable of resolving with its approximately 7 km x 7 km spatial resolution.

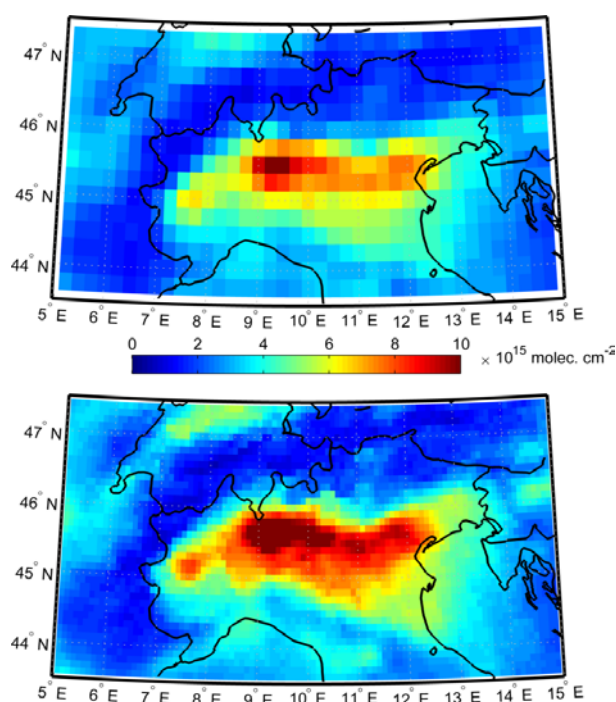


Figure 24: Comparison of the standard resolution (top) and high-resolution (bottom) OMNO2e product, shown here for Northern Italy.

3.3.3 Time series

NO₂

Automated methods for extracting combined time series from all available sensors have been developed. This allows the extraction of a 17-year time series for NO₂

(1995-2012) and a 10-year time series for SO₂ (2002-2012) at any point on the globe simply by specifying coordinates. Time series have been computed for several of the major urban areas in the EECCA region. Figures 25 through 30 show examples of time series extracted from the four EO instruments over several major urban areas within the EECCA countries, namely Moscow, Minsk, Kiev, Tbilisi, Yerevan and Baku.

The scarcity of in situ data within the EECCA region and the additional temporal information that satellite data can provide is illustrated in Figure 31.

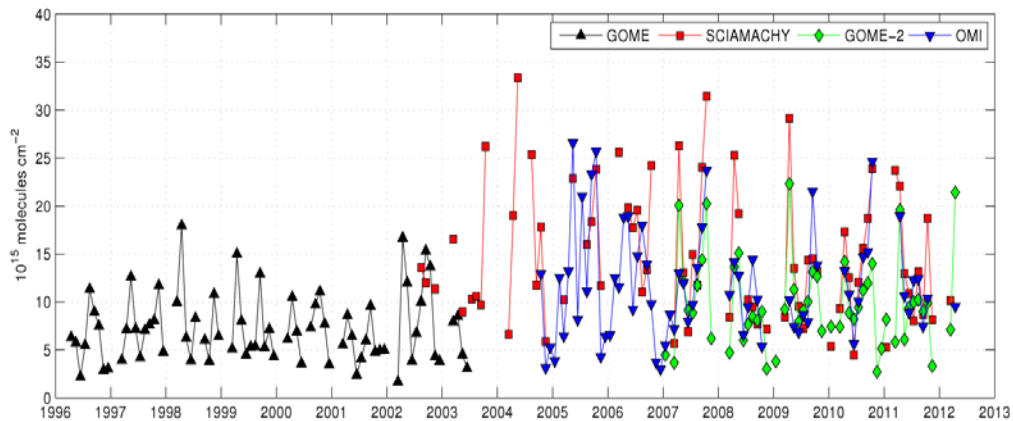


Figure 25: Time series of NO₂ over Moscow (55.75°N, 37.62°E) extracted from monthly data from all four instruments. The extraction was carried out as the average of a 3 x 3 array of grid cells.

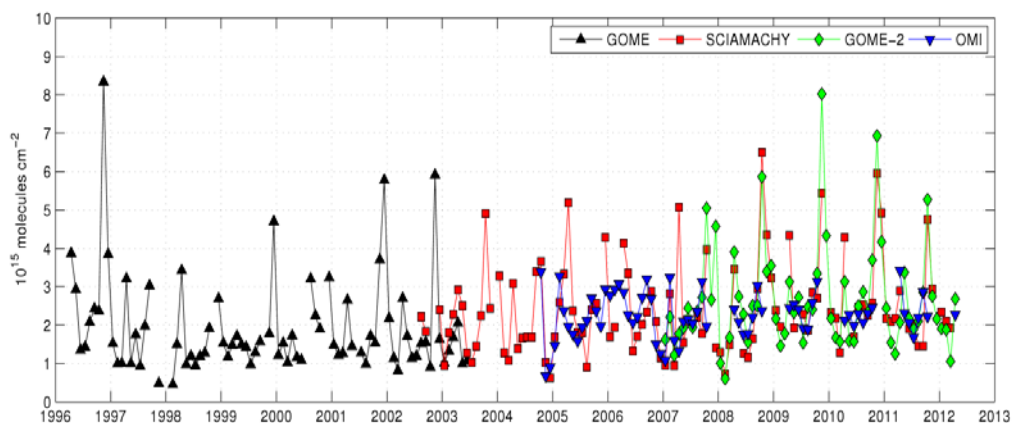


Figure 26: Time series of NO₂ over Minsk (53.89°N, 27.56°E) extracted from monthly data from all four instruments. The extraction was carried out as the average of a 3 x 3 array of grid cells.

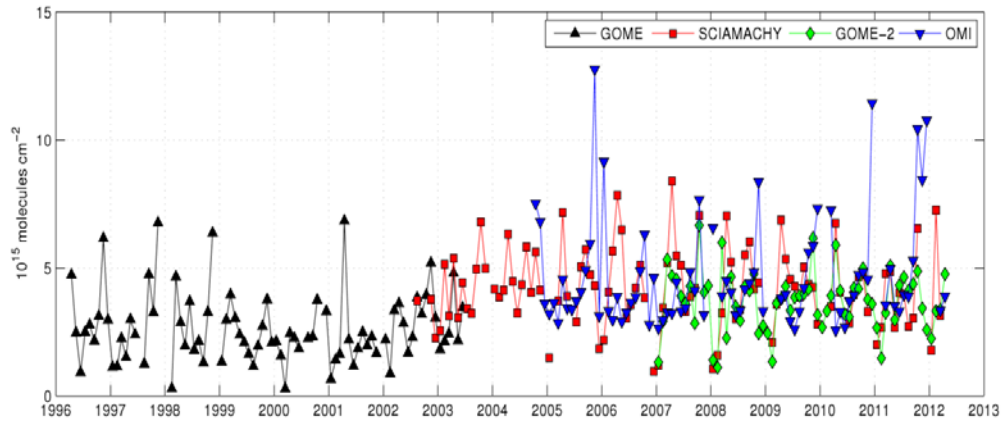


Figure 27: Time series of NO₂ over Kiev (50.442°N, 30.528°E) extracted from monthly data from all four instruments. The extraction was carried out as the average of a 3 x 3 array of grid cells.

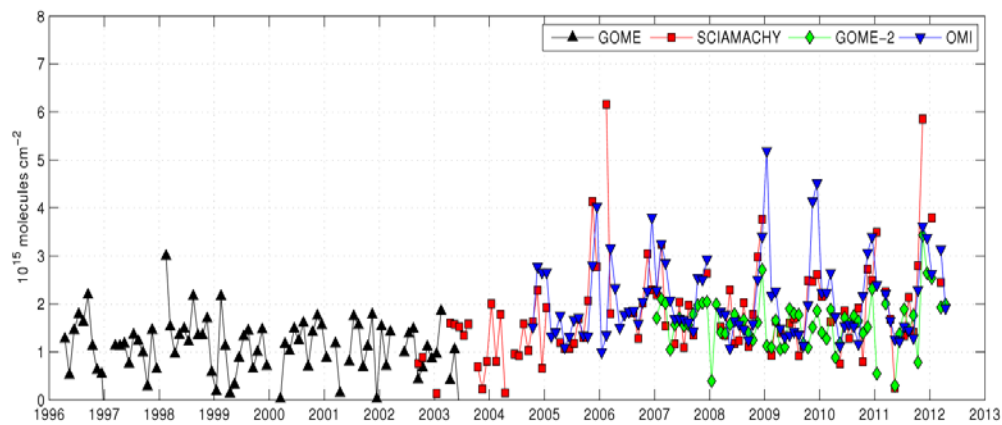


Figure 28: Time series of NO₂ over Tbilisi (41.711°N, 44.789°E) extracted from monthly data from all four instruments. The extraction was carried out as the average of a 3 x 3 array of grid cells.

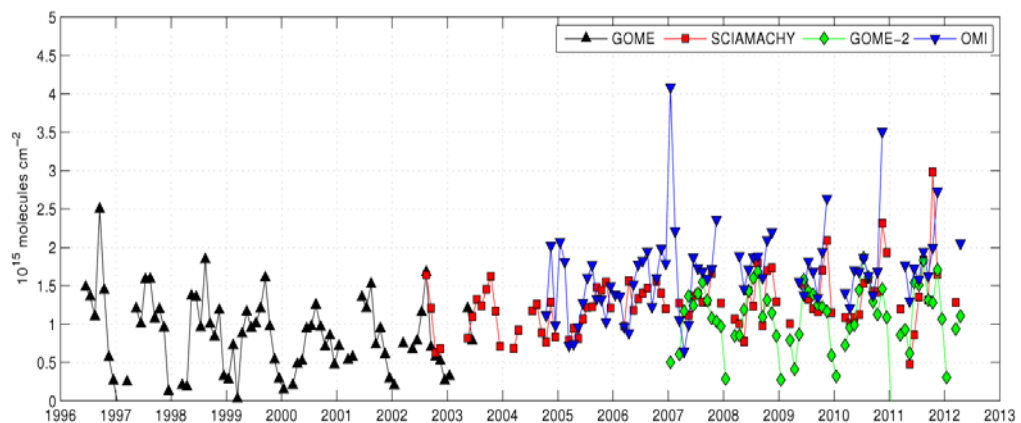


Figure 29: Time series of NO₂ over Yerevan (40.183°N, 44.514°E) extracted from monthly data from all four instruments. The extraction was carried out as the average of a 3 x 3 array of grid cells.

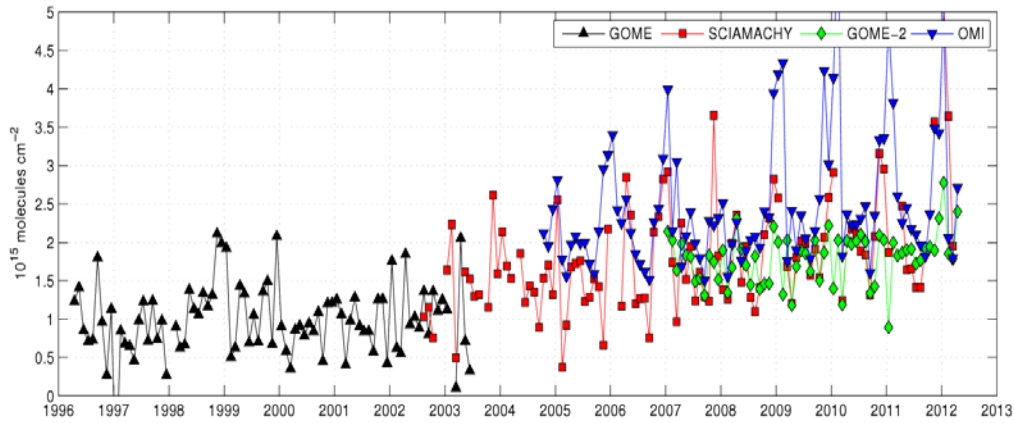


Figure 30: Time series of NO₂ over Baku (40.41°N, 49.84°E) extracted from monthly data from all four instruments. The extraction was carried out as the average of a 3x3 array of grid cells.

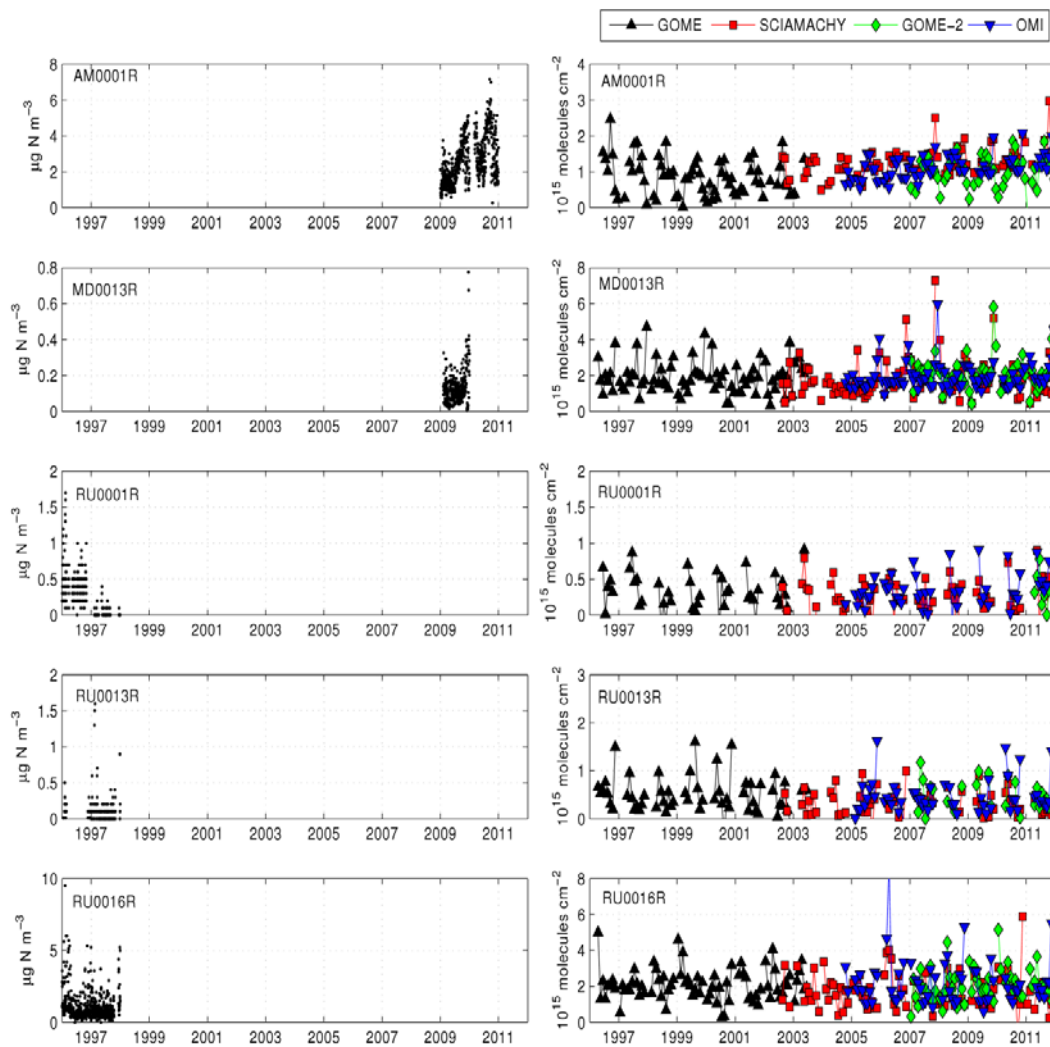


Figure 31: Comparison of all (!) available NO₂ ground station data available within the EMEP network within the entire EECA area as acquired from the EBAS database (left column) and time series of tropospheric column NO₂ EO data acquired over the same locations.

SO₂

Additional investigations of sulfur dioxide (SO₂) products were carried out. A general problem with SO₂ products from space is that the algorithms used in the process often deliver negative values. This makes the quantitative use of the SO₂ tropospheric columns challenging and mostly limits the products' applications to studying spatial patterns and temporal behavior.

In particular, a closer look at SO₂ products was taken at the Norilsk region in Northern Russia. This industrial area includes the world's largest Nickel mine and smelter and as such is responsible for ca. 1% of all global emissions of SO₂ as well as approximately 10% of all European SO₂ emissions. Figure 32 shows a map of the long-term mean SO₂ concentration in the Norilsk region, computed from 2002-2012 SCIAMACHY data. A time series was extracted over a 3 by 3 pixel region centered of the Norilsk smelter and is shown in Figure 33. A weak seasonal cycle with a minimum during the winter months and a summer maximum can be identified.

As another example of what kind of SO₂ source can be detected from space, Figure 34 shows long-term average SO₂ concentration over Romania, in this case computed from daily OMI SO₂ observations provided by NASA. One very strong hotspot can be found over the southwestern part of the country. This hotspot is associated with the Rovinari power plant located at 44°54' N and 23°8' E.

Again, it can be seen in all of these Figures that negative values are provided by the product. This has been found for different SO₂ products derived from both SCIAMACHY and OMI.

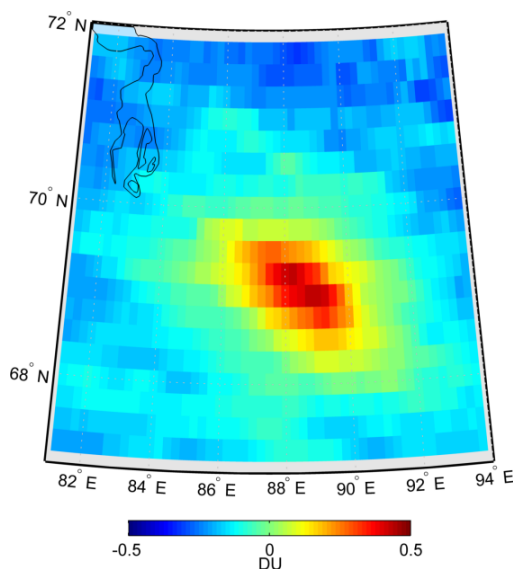


Figure 32: Long-term mean SO₂ column for the area of the Norilsk nickel smelter in Northern Russia, derived from the 2004-2012 SCIAMACHY monthly mean dataset

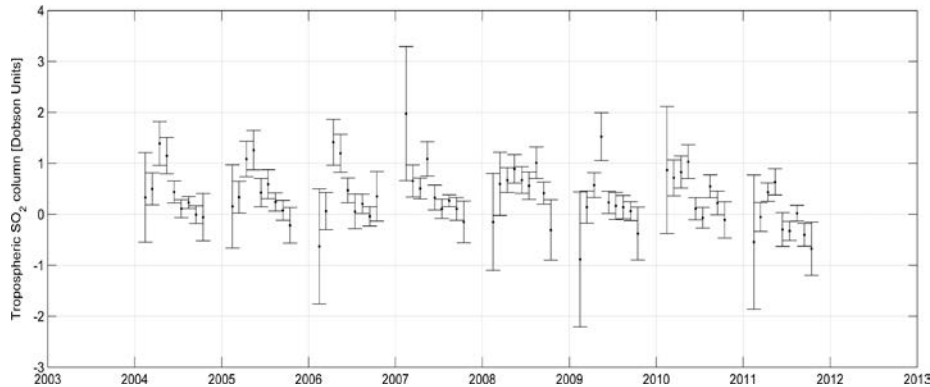


Figure 33: Time series of SCIAMACHY-derived SO_2 column and the associated uncertainty for the area of the Norilsk nickel smelter in Northern Russia. The time series was derived from a 3×3 pixel array centered over Norilsk.

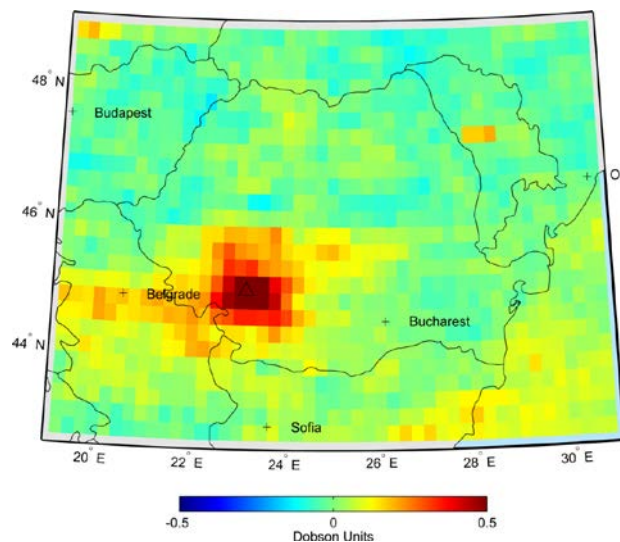


Figure 34: 2005-2011 mean SO_2 column over Romania derived from daily OMI data (OMS02e product). Clearly visible is the SO_2 hotspot over the power plant in the southwest of Romania. Note that due to interference with ozone within the retrieval algorithm the SO_2 columns can obtain slightly negative values.

Trend analysis for NO_2

Based on the methodology shown by Schneider and van der A (2012) the magnitude of the long-term trends of the tropospheric nitrogen dioxide columns were calculated over the EECCA region using data acquired by the SCIAMACHY instrument between 2002 and 2012. The trend analysis is based on fitting a statistical model to the time series, which incorporates a seasonal component. Figure 35 shows the result for a subset of the EECCA region. Note that only trends significant at the 95% level are shown.

The spatial patterns of the found statistically significant trends are not consistent and made up of mostly scattered data points throughout the study region though coherent clusters are visible in some cases. Mostly increasing levels of NO_2 can

be found in the western part of Russia, in particular along the border to Ukraine and Belarus. Many parts of this region exhibit significantly increasing concentrations of tropospheric NO₂ with relative growth rates of 3% per year and more, reaching maximum levels of up to 10% per year.

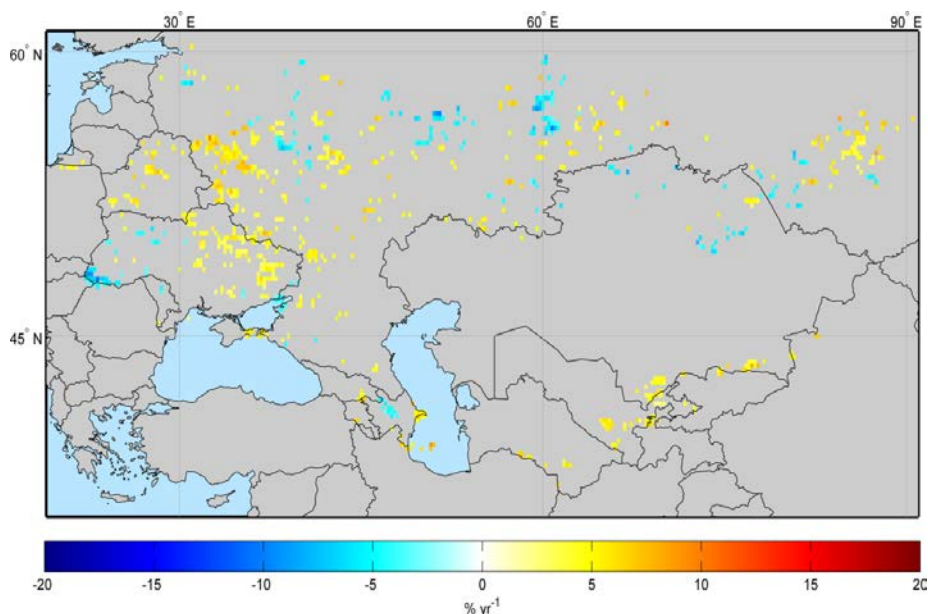


Figure 35: Relative trends in the tropospheric nitrogen dioxide column acquired by the SCIAMACHY instrument between 2002 and 2012. Only trends significant at the 95% level are shown. The methodology is described in detail in Schneider and van der A (2012)

3.4 Conclusions

While the existing NO₂ products mostly agree on spatial patterns, they can vary quite substantially in terms of actual concentrations at the pixel level. When using NO₂ data from multiple instruments and in particular when creating long time series, it is therefore highly recommended to use a consistent algorithm throughout. At the moment, this can be most easily accomplished by using data from www.temis.nl, which provides daily and monthly NO₂ products from all four major instruments derived with a consistent algorithm and methodology.

Even when doing so, it is recommended to be very cautious when merging and comparing data from multiple instruments, since changes in spatial resolution between sensors (in particular when using the 320 x 40 km GOME footprint together with more modern instruments) as well as varying local overpass times can still result in significant differences between NO₂ retrievals and complicate the generation of real geophysical trends from multiple instruments.

As far as SO₂ is concerned, the currently available products can be helpful for mapping SO₂ at continental and global scales and for detecting some emission hotspots. Generally, only very strong emissions of SO₂ can be detected, which is why the products are most useful for providing aviation with advice on volcanic eruptions. Very strong anthropogenic emissions such as over Eastern China or the Norilsk nickel smelter in Russia can also be detected as spatial patterns in images

averaged over several months. However, it is currently not recommended to use any of the official products for actually quantifying anthropogenic SO₂ levels.

3.5 References

- Boersma, K. F., Eskes, H. F., and Brinksma, E. J. (2004). Error analysis for tropospheric NO₂ retrieval from space. *Journal of Geophysical Research*, 109(D4).
- Boersma, K. F., Eskes, H. J., Dirksen, R. J., van der A, R. J., Veefkind, J. P., Stammes, P., Huijnen, V., Kleipool, Q. L., Sneep, M., Claas, J., Leit˜ao, J., Richter, A., Zhou, Y., and Brunner, D. (2011). An improved tropospheric NO₂ column retrieval algorithm for the Ozone Monitoring Instrument. *Atmospheric Measurement Techniques*, 4:1905--1928.
- Boersma, K. F., Eskes, H. J., Veefkind, J. P., Brinksma, E. J., van der A, R. J., Sneep, M., van den Oord, G. H. J., Levelt, P. F., Stammes, P., Gleason, J. F., and Bucsela, E. J. (2007). Near-real time retrieval of tropospheric NO₂ from OMI. *Atmospheric Chemistry and Physics*, 7:2103--2118.
- Bovensmann, H., Burrows, J. P., Buchwitz, M., Frerick, J., Noˆel, S., Rozanov, V. V., Chance, K. V., and Goede, a. P. H. (1999). SCIAMACHY: Mission Objectives and Measurement Modes. *Journal of the Atmospheric Sciences*, 56(2):127--150.
- Burrows, J. P., Weber, M., Buchwitz, M., Rozanov, V., Ladstˆatter-Weiˆß en-mayer, A., Richter, A., DeBeek, R., Hoogen, R., Bramstedt, K., Eichmann, K.-U., Eisinger, M., and Perner, D. (1999). The Global Ozone Monitoring Experiment (GOME): Mission Concept and First Scientific Results. *Journal of the Atmospheric Sciences*, 56(2):151--175.
- Callies, J., Corpaccioli, E., Eisinger, M., Hahne, A., and Lefebvre, A. (2000). GOME-2 - Metop's Second-Generation Sensor for Operational Ozone Monitoring. *ESA Bulletin*, 102:28--36.
- Dentener, F., van Weele, M., Krol, M., Houweling, S., and van Velthoven, P. (2003). Trends and inter-annual variability of methane emissions derived from 1979-1993 global CTM simulations. *Atmospheric Chemistry and Physics*, 3:73--88.
- Gottwald, M., Bovensmann, H., Lichtenberg, G., Noel, S., von Bargaen, A., Slijkhuis, S., Pitters, A., Hoogeveen, R., von Savigny, C., Buchwitz, M., Kokhanovsky, A., Richter, A., Rozanov, A., Holzer-Popp, T., Bramstedt, K., Lambert, J.-C., Skupin, J., Wittrock, F., Schrijver, H., and Burrows, J. (2006). SCIAMACHY - Monitoring the Changing Earth's Atmosphere. DLR, Institute fuer Methodik der Fernerkundung (IMF).
- Levelt, P., van den Oord, G., Dobber, M., Malkki, A., Stammes, P., Lundell, J., and Saari, H. (2006). The Ozone Monitoring Instrument. *IEEE Transactions on Geoscience and Remote Sensing*, 44(5):1093--1101.
- Munro, R., Eisinger, M., Anderson, C., Callies, J., Corpaccioli, E., Lang, R., Lefebvre, A., Livschitz, Y., and Albinana Perez, A. (2006). GOME-2 on MetOp. In *Proceedings of the 2006 EUMETSAT Meteorological Satellite Conference*, Helsinki, Finland.
- Richter, A. and Burrows, J. P. (2002). Tropospheric NO₂ from GOME measurements. *Advances in Space Research*, 29(11):1673--1683. Richter, A., Heckel, A., Oetjen, H., Wittrock, F., and Burrows, J. P. (2006). Using GOME-2 Measurements to extend the GOME/SCIAMACHY tropospheric NO₂ record. In *Proceedings of the 1st EPS/MetOp RAO Workshop (15-17 May 2006)*, Frascati, Italy.

Schneider, P., van der A, R.J., 2012. A global single-sensor analysis of 2002-2011 tropospheric nitrogen dioxide trends observed from space. *Journal of Geophysical Research* 117, 1–17.

van Geffen, J. (2008). Volcanic & Air Quality SO₂ Service Product Information. Technical report.

Appendix A

Glantz et al., poster, CRAICC meeting, 2012

Paul Glantz*, Matthias Tesche*, Hamish Struthers* and Kerstin Stebel*
 *Department of Applied Environmental Science (ITM), Stockholm University
 *Norwegian Institute for Air Research (NILU), Kjeller, Norway

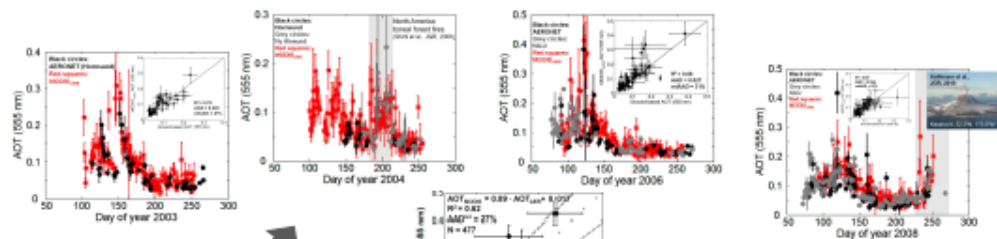
contact: paul.glantz@itm.su.se

INTRODUCTION

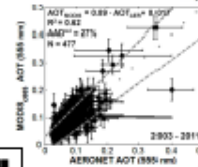
Due to ice-albedo feedback the Arctic is expected to be the region on Earth that is most sensitive to global warming. On the other hand, increased area of open water surfaces mean that emissions of sea salt and organic aerosol as well as DMS are expected to increase significantly in the future. It is therefore important to include these sources of aerosols in regional and global climate model simulations to estimate impacts on the radiation balance. However, the models need to be validated against ambient conditions, which is possible based on remote sensing of aerosols in the atmosphere. By introducing MODIS₀₃₀₃ retrievals of AOT over the area around Svalbard, substantially better time coverage (~75%), compared to ground-based sun-photometer data (~30%), is obtained for the subarctic marine region. Hence, short- and long-term variations in AOT can be investigated with better accuracy.

CONCLUSIONS

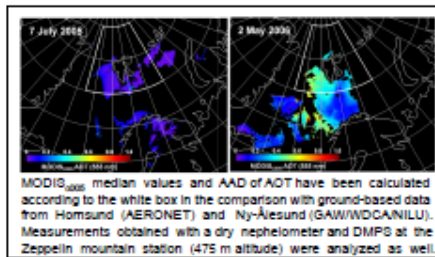
- MODIS₀₃₀₃ AOT were found to be within 30% of the ground-based estimates and, for values lower than 0.2, on the whole within the expected uncertainty range of MODIS retrievals over ocean surfaces
- A positive trend in MODIS AOT is found for June when the present investigation period was compared to the previous years 1995 - 1999
- In comparison with MODIS retrievals it was found that AOT estimated with CAM3-Oslo is overestimated by a factor of 3 in summer and fall, most likely due to unrealistic long-range transport of aerosols in the model
- The long-term in-situ measurements of dry scattering coefficient at the Zeppelin mountain station give a bad representation of aerosol scattering, particularly in summer when high relative humidity occurs



MODIS₀₃₀₃ AOT validated against ground-based sun-photometer data



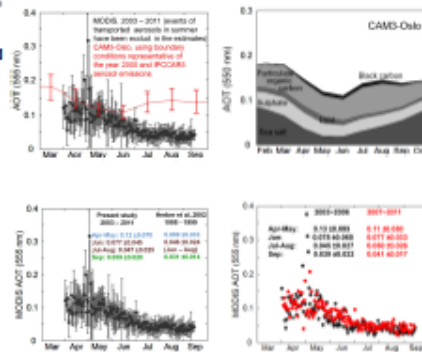
Time coverage (median values) of MODIS daily AOT (2003-2011):
 April - May: 72%
 June: 80%
 July - August: 79%
 September: 27%



MODIS₀₃₀₃ median values and AAD of AOT have been calculated according to the white box in the comparison with ground-based data from Homsund (AERONET) and Ny-Alesund (GAW/WDCA/NILU). Measurements obtained with a dry nephelometer and DMPS at the Zeppelin mountain station (475 m altitude) were analyzed as well.

How accurately is arctic AOT simulated by the CAM3-Oslo global model?

Long-term trend in MODIS AOT?



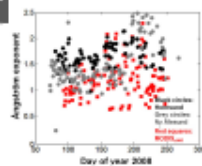
How representative are the current long-term dry measurements of aerosol scattering at the Zeppelin mountain station?

List of shortening

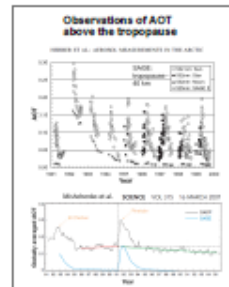
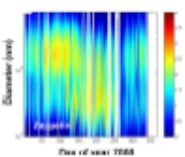
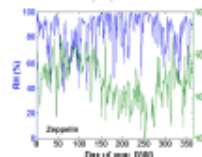
- AAD Absolute average Deviation
- AERONET Aerosol Robotic Network
- AOT Aerosol optical thickness
- CO2S Collection 5
- DMPS Differential mobility particle sizer
- GAW Global Atmospheric Watch
- MODIS Moderate resolution imaging Spectroradiometer
- WDCA World Data Centre for Aerosols

Dashed lines in the scatter figure denote expected uncertainties of the MODIS retrievals

Supported by the Swedish Research Council VR and FORMAS



"By assuming a boundary layer height of 2 km, and homogenous aerosol conditions, measurements with the dry nephelometer give an AOT as low as 0.002 in summer"



Appendix B

Chapter 6.5 of Myhre et al. (2012)

6.5 Utilization of satellite data as a complement to aerosol observations above Scandinavia and the European Arctic

Despite relative high uncertainties of satellite aerosol products in the Arctic, the use of earth-observation (EO) data in polar region is steadily increasing. Beside total column measurements, the global 3-D distribution of tropospheric aerosols can be nowadays characterized from satellite data, like the CALIOP lidar (see Winker et al., 2012). As another example for utilization of EO data in the Arctic, we can mention the work of Sodemann et al. (2011), describing episodes of cross-polar transport in the Arctic troposphere during July 2008 as seen from models, satellite, and aircraft observations. The authors use CO from the IASI passive infrared sensor on-board the MetOp-A satellite and aerosol backscatter and depolarization from the CALIPSO satellite; Kristiansen et al. (2010) use SO₂ columns from GOME-2, OMI, and AIRS, and total attenuated backscatter at 532 nm and 1064 nm (level 1B data) from CALIOP, to study the transport of the Kasatochi (52.2°N, 175.5°W) eruption sulfur dioxide cloud on 7 to 8 August 2008, leading to an increase of total aerosol column above Ny-Ålesund in August and September 2008.

Before embedding earth observation data into National monitoring activities, their quality and added value has to be accessed, as the retrievals are generally not tuned to polar and high latitude regions. A poster presentation by Glantz et al. (2012) showed that by introducing MODISc005 retrievals of aerosol optical density (AOD) over the area around Svalbard substantially better time coverage (~75%), compared to ground-based sun-photometer data (~30%) is obtained for the Subarctic marine region. MODISc005 AOD was found to be within 30% of the ground-based estimates and, for values lower than 0.2, on the whole within the expected uncertainty range of MODIS retrievals over ocean surfaces.

As an example, in Figure 47, we show a comparison of daily averaged aerosol optical depth (AOD) data within ± 2 degrees from Ny-Ålesund and Palgrunden (a South-Swedish AERONET site), from the Advanced Along-Track Scanning Radiometer AATSR, which have been developed in the framework of ESA's AEROSOL-CCI project: AATSR SU 4.0 (developed at Swansea University), AATSR ADV v1.42 (developed at the Finnish Meteorological Institute), and AATSR ORAC v. 2.02 (developed at University of Oxford). A full year data set – 2008 – is available, for details see: www.esa-aerosol-cci.org.

A rough assessment of the suitability of the individual retrievals for the Norwegian National monitoring would conclude that the AATSR ORAC v. 2.02 would be the most promising choice. The cut-off for AATSR SU 4.0 is around 70°N and no data are available for the region around Svalbard. The general seasonal pattern seen in Ny-Ålesund seems nicely reproduced by AATSR ADV v1.42, but the retrieved AOD values seem underestimated. A correlation of 0.52 (Ny-Ålesund) and 0.66 (Palgrunden) is obtained by using data from AATSR ORAC v. 2.02.

In Figure 48a/b we show the monthly averaged data from AATSR ORAC v. 2.02 (left panel) and the AOD observations from the ground-based AERONET

network (plus Ny-Ålesund), as reported in Toledano et al. (2012). Due to lack of sun, no data are available for the month of January and December 2008. It is obvious that the satellite data are adding the spatial information not covered by ground-based observations from Ny-Ålesund and Birkenes (started in 2009), which are the two sites at present funded via Klif's monitoring program. Nevertheless, further analysis is needed to access the added value of these observations, e.g. can they be used for correctly described inter-annual variability and trends. A multi-annual data will be provided through ESA's AEROSOL-CCI project in 2013. If available in time, trend studies utilizing this long-term average will be results included in the 2013 annual monitoring report.

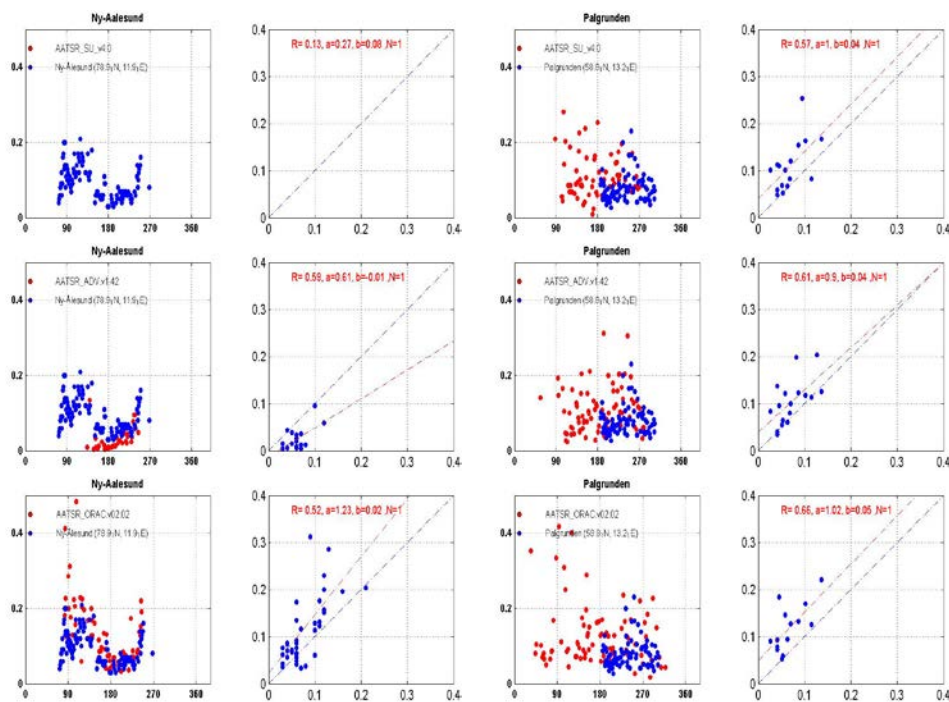


Figure 47: Time-series and comparison of daily average aerosol optical depth measured from satellite around Ny-Ålesund and Palgrunden during the sunlight time periods in 2008. The satellite data are averaged within ± 2 degrees around the stations. Shown are retrievals from AATSR, which have been developed in the framework of ESA's AEROSOL-CCI project: AATSR SU 4.0 from Swansea University (upper panel), AATSR ADV v1.42 from the Finnish Meteorological Institute (middle panel), and AATSR ORAC v. 2.02 from University of Oxford (lower panel).

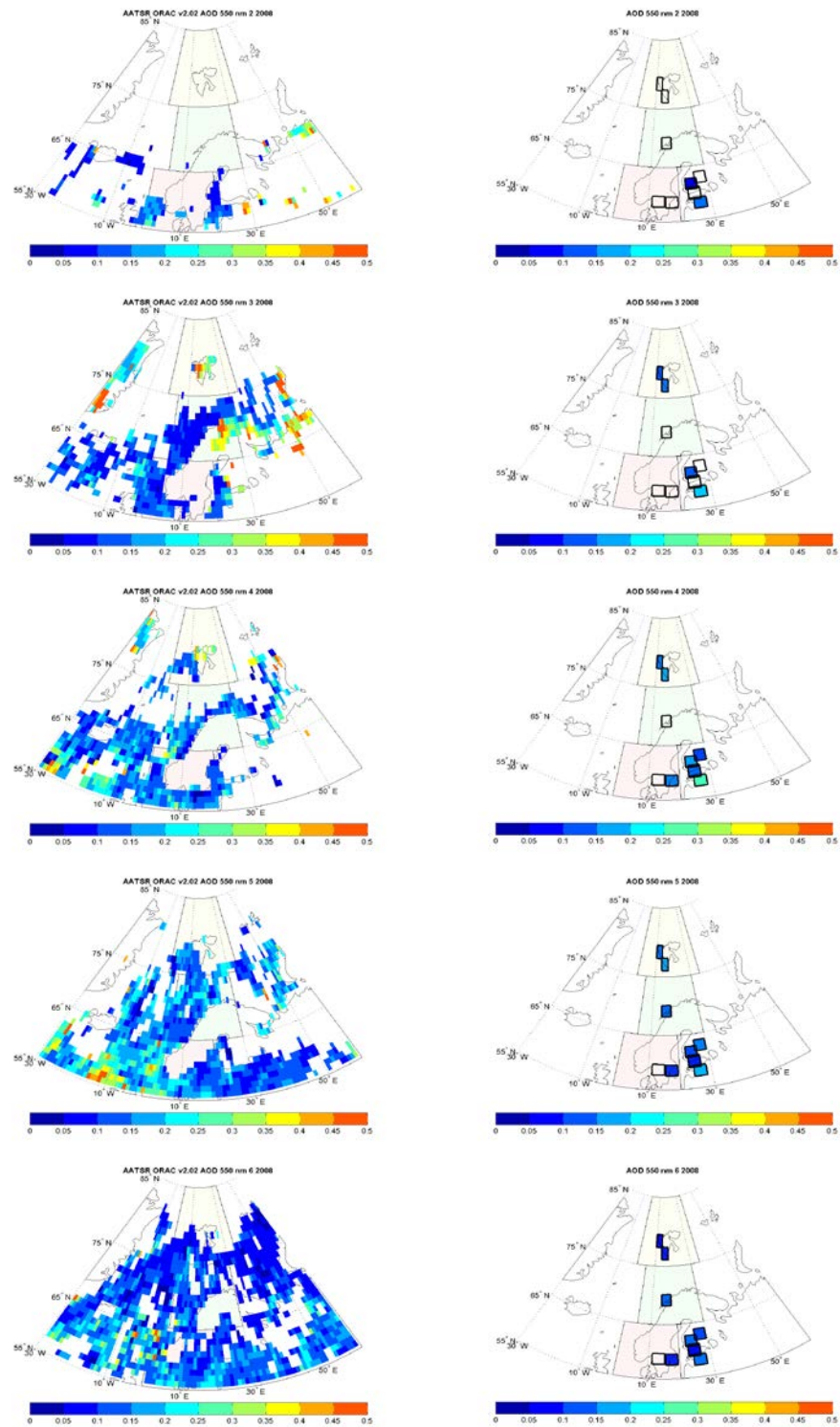


Figure 6 a: Monthly mean aerosol optical depth measured from the AATSR satellite, AATSR ORAC v. 2.02 from University of Oxford, and ground-based AOD network (see Toledano et al., 2012). Shown are the month February – June 2008.

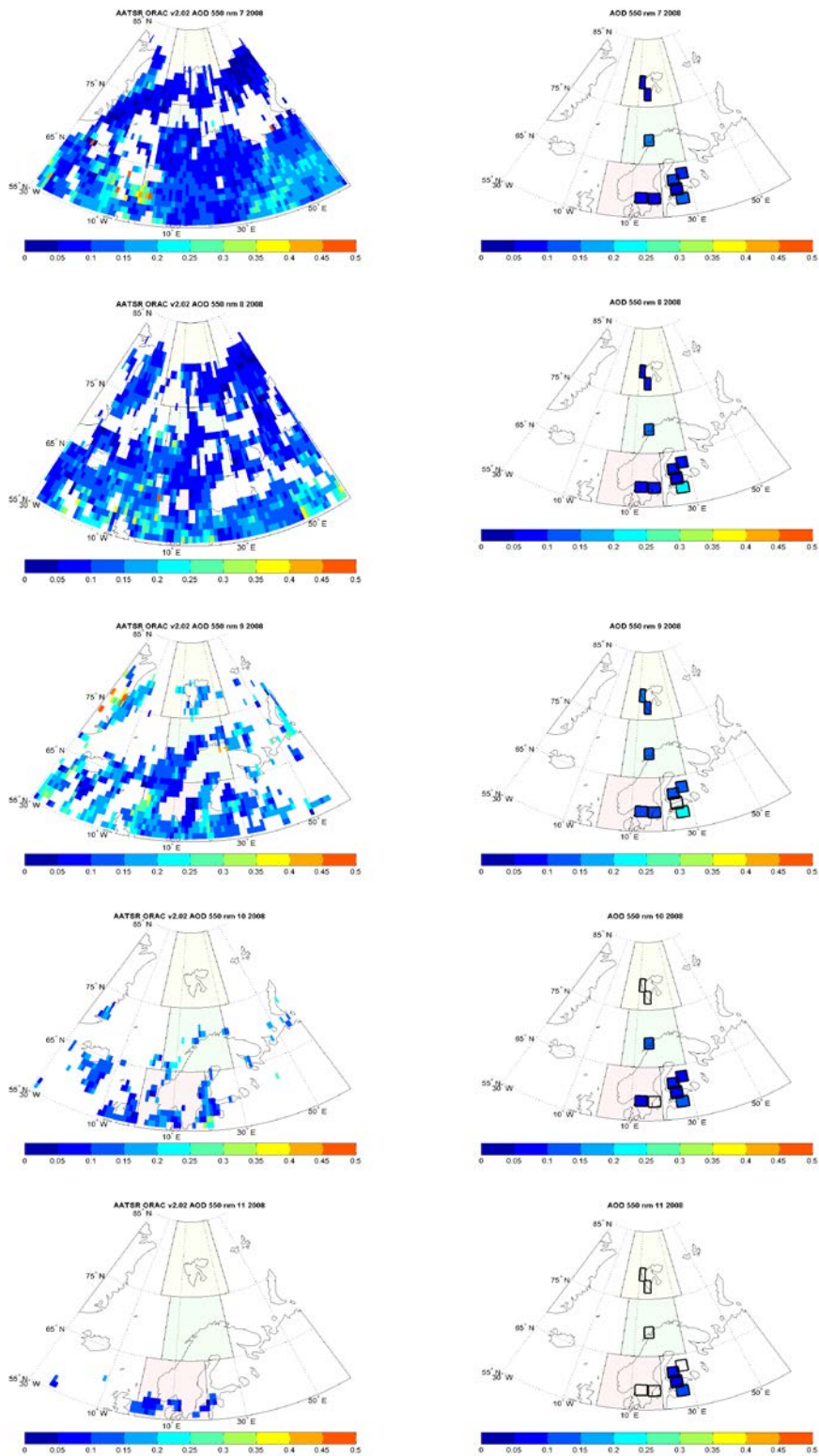


Figure 6 b: Monthly mean aerosol optical depth measured from the AATSR satellite, AATSR ORAC v. 2.02 from University of Oxford, and ground-based AOD network (see Toledano et al., 2012). Shown are the months July – November 2008.

As a final example, in Figure 49 monthly mean aerosol extinction profiles from the CALIOP lidar are shown. Night-time monthly averaged Level 3 data are plotted. Combined data (cloud free + above cloud) with horizontal resolution of $5^\circ \times 2^\circ$ (longitude \times latitude) and a vertical resolution of 60 m are given (CAL_LID_L3_APro_AllSky-Beta-V1-00). For details see http://eosweb.larc.nasa.gov/PRODOCS/calipso/table_calipso.html for more details). The data are averaged within the 3 areas, indicated in Figure 2, representative for Svalbard, Northern and Southern Norway. The profiles shown cover the time period from June 2006 to November 2012. Clearly, the contribution of the volcanic aerosol to the total aerosol load in autumn 2008 can be seen. In addition a lower boundary for the aerosol layer is seen above Svalbard. Furthermore, a seasonal cycle in the lower troposphere, related to Arctic haze, is seen. In-depths analysis is still outstanding, and will be presented in the 2013 report.

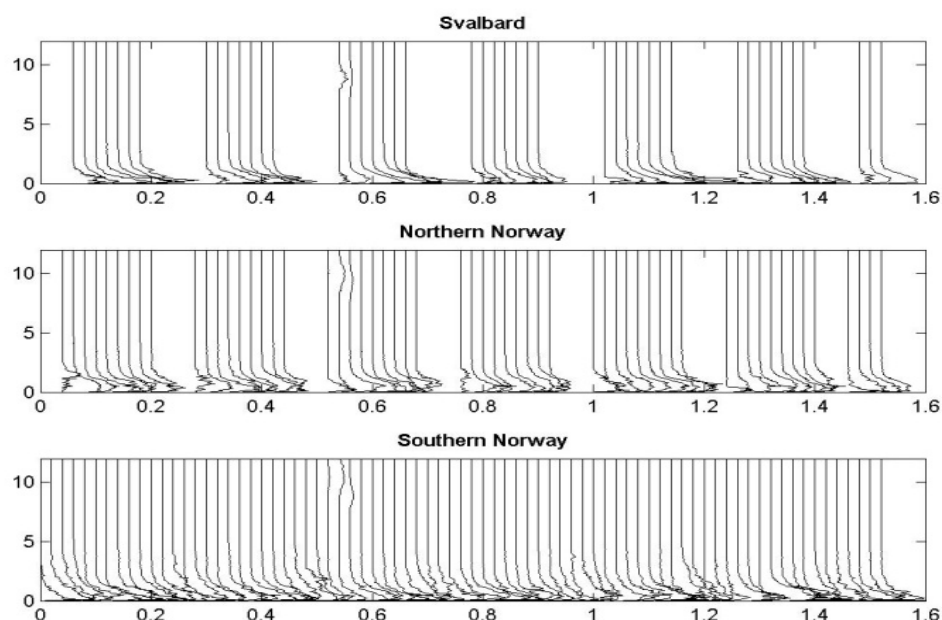


Figure 49: Monthly mean night-time aerosol extinction profile, averaged within 3 areas (upper panel: latitude $[75^\circ\text{N} - 85^\circ\text{N}]$, longitude $[-0^\circ\text{E} - 35^\circ\text{E}]$; middle panel: latitude $[65^\circ\text{N} - 75^\circ\text{N}]$, longitude $[5^\circ\text{E} - 30^\circ\text{E}]$ and lower pane: latitude $[55^\circ\text{N} - 65^\circ\text{N}]$, longitude $[0^\circ\text{E} - 20^\circ\text{E}]$). Profiles from the June 2006 until November 2012 are shown.

Appendix C

Chapter 5.1 of Myhre et al. (2012)

5.1 Analysis of CO from satellite observations to support ground based measurements at Birkenes

CO is a component of particular importance as tracer for biomass burning and knowledge of this compound is important for the understanding of sources and levels of both to aerosols (see chapter 6) and gases like CH₄ and CO₂. Ground based monitoring of this compound is lacking in Norway, and only available at Svalbard far from fire sources. Based on a project financed by The Norwegian Space Centre (NRS) (Norsk Romsenter, <http://www.romsenter.no/>) we are now in a position where we can support the national monitoring of greenhouse gases and aerosols by exploring and utilize satellite observations of CO. The project, *SatMonAir*, started in January 2012 and ended December 2012. A new project following up the work is starting January 2013, and NRS is highly acknowledged for their support. The results from this work are included in this report (also in section 6.5 at page 67).

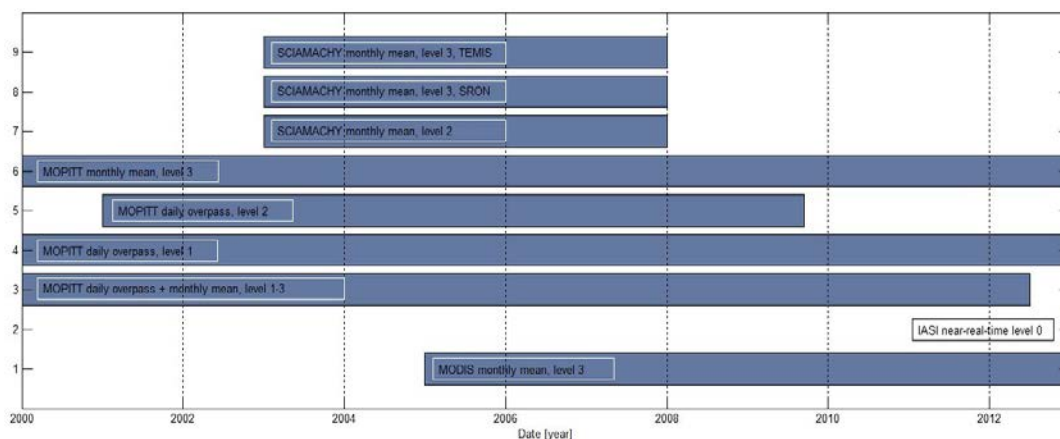


Figure 34: EO-based CO data of particular importance for national monitoring to KLIF.

The goal of this work is twofold; setting up an alert system to follow fires and possible influence on the observations in near real time, and secondly support the analysis of aerosols (particularly the absorbing aerosol) and the CO₂ and CH₄. Not all the above listed products are well suited for our purpose. The availability of data in time and space does in some cases not cover the region or the years of interest, and while investigating the available products in detail, we also discovered that the routines for searching, online plotting and download of data might not be straight forward.

A simple web page serves provides links to the relevant trace gas products, set up for internal use at <http://zardoz.nilu.no/~annm/satmonair/> and <http://zardoz.nilu.no/~annm/satmonair/plots/fires.html>. The web pages does not only contain a list of EO products used, but also URLs to online fire products provided by FIRMS (Fire Information for Resource Management System) <http://earthdata.nasa.gov/data/near-real-time-data/firms>. We have been using the products from FIRMS to investigate the number of fires in the Eastern Europe and

Russian areas in the spring, as these are relevant regions for long-range transport of aerosols to Norway and Scandinavia.

Examples of global fire maps are shown in Figure 35. This will be further dealt with in the follow-up project in 2013.

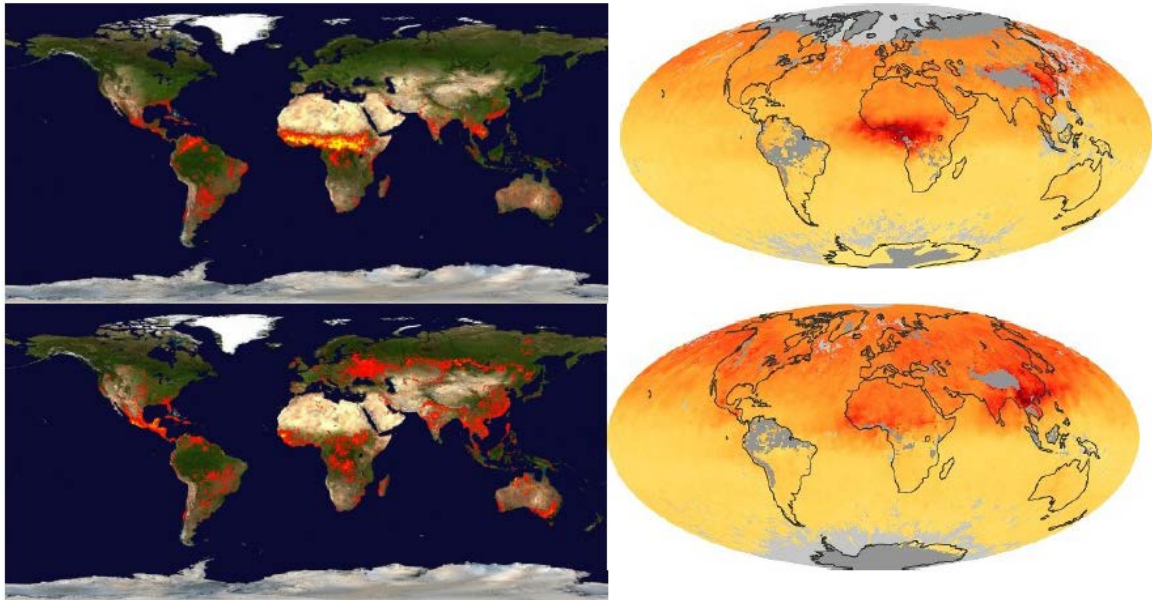


Figure 35 : Left panel: The geographical locations of all hot spots detected by MODIS on 11.-20 January 2011 (upper panel) and 21.-30 May 2011 (lower panel). Right panel: Monthly average CO for January 2011 (upper panel) and May 2011 (lower panel) from MOPITT.

The Figure show that in the northern hemisphere winter there are very few fires in the Eastern Europe and Russian Areas, and the CO the right, whilst spring shown in the lower panel, is an active season for natural fires in the Eastern Europe and Russian Areas.

We have further investigated high aerosol episodes in the Arctic and Scandinavian areas in the years 2004-2011 with special emphasis on 2011. In 2011 there were very few episodes at both Birkenes and Zeppelin influenced by direct emissions from fires, partly due to the meteorology mainly with prevailing winds from west in the spring season. This work will continue and be further developed in 2012 and 2013.

Appendix D

Chapter 4 of Svendby et al. (2012)

Chapter 4 : Satellite observations of ozone above Norway and the Norwegian Arctic region

Satellites can never replace our ground based ozone monitoring network, but they give a very important contribution to the global ozone mapping. For Norway and the Arctic the use of satellite data will provide valuable information on spatial distribution of ozone and UV radiation. Satellites also make it possible to investigate the geographical extent of low ozone episodes during spring and summer and thereby discover enhanced UV intensity on a regional level. Based on projects jointly financed by The Norwegian Space Centre (NRS) (Norsk Romsenter) and NILU we are in a good position to explore and utilize ozone satellite observations in the National monitoring of the ozone and UV radiation. One project (SatLuft) started in October 2007 and ended late 2010. Another project (SatMonAir) started in 2012. Some results from the activities within the ongoing SatMonAir project are included in this report.

4.1 Short introduction to ozone observations from space

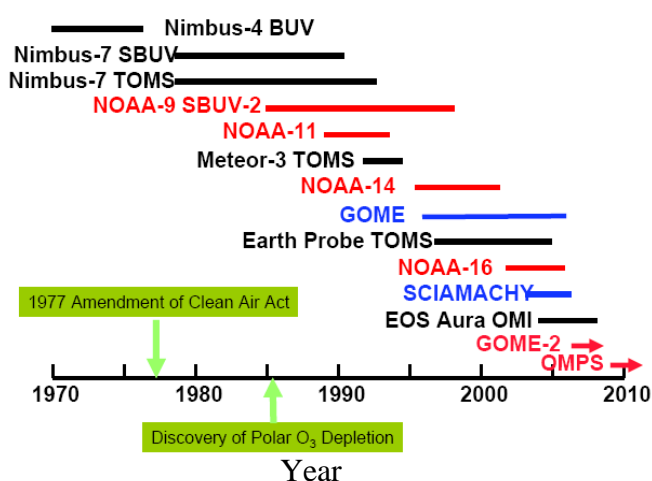


Figure 14: An overview of the various satellites and their instruments measuring ozone from space since the beginning of 1970's (Figure from NASA).

determining the daily ozone levels. Thus, observing ozone fluctuations over just one spot is not sufficient to give a precise description of the ozone situation in a larger region. Satellite observations are filling these gaps. However, satellite observations rely on proper ground based monitoring as satellites have varying and unpredictable life times, and calibration and validation rely on high quality ground based observations. Thus satellite observations are complementary to ground based observations, and both are highly necessary.

Observations of seasonal, latitudinal, and longitudinal ozone distribution from space have been performed since the 1970's, using a variety of satellite instruments. The American institutions NASA and NOAA (National Oceanic and

The amount and distribution of ozone in the stratosphere varies greatly over the globe and is mainly controlled by two factors: the fact that the maximum production of ozone takes place at 40 km height in the tropical region, and secondly the large scale stratospheric transport patterns towards the mid- and high latitudes. In addition there are small scale transport and circulation patterns in the stratosphere

Atmospheric Administration) started these observations, and later The European Space Agency initiated their ozone programmes.

4.2 Satellite ozone observations above the Norwegian sites from 1978–2011

In the course of the last 35 years several satellites have provided ozone data for Norway. The most widely used instruments have been TOMS (onboard Nimbus-7), TOMS (onboard Meteor-3), TOMS (on Earth Probe), GOME I (on ESR-2), GOME-2 (on MetOp), SCIAMACHY (on Envisat), and OMI (onboard Aura). Figure 14 shows the life time of the various satellites. In the 1980s TOMS-Nimbus 7 was the only satellite borne ozone instrument in space, but the last decades overlapping ESA and NASA satellite products have been available. Also, different ozone retrieval algorithms have been used over the years, which have gradually improved the quality and confidence in the ozone data. Corrections for instrumental drift and increased knowledge of ozone absorption cross sections and latitude dependent atmospheric profiles have improved the data quality, especially in the Polar region.

In section 3.5 we describe the special ozone situation in the spring 2011, where very low ozone values were measured until the beginning of April. Figure 15 (left panel) and Figure 15 (right panel) show the Scandinavian/Arctic ozone situation 1st April 2011 and 1st April 2010, respectively. The ground based Brewer ozone values for Oslo and Andøya are marked in the figures (blue numbers) along with the OMI ozone value at the same locations (black numbers). As seen from the two figures the colours are very different. In the beginning of April 2010 the Arctic ozone level was close to the long term mean, whereas the large 2011 ozone depletion is visualized by the light blue colours in Figure 15 (left panel). Comparisons between Brewer and OMI data over Oslo and Andøya show that the satellite values differs by some Dobson Units from the ground based measurements. Ozone can exhibit some variations within short distances and an OMI satellite pixel of 1x1 degree might have an average value that deviates from the point measurement. On the other hand the satellites give a very good picture of spatial extent of the “ozone hole” and how ozone rich/poor air moves. As a part of the SatMonAir project spatial correlation, standard deviation and bias between satellite products (plus comparisons to ground based measurements) will be studied in more detail.

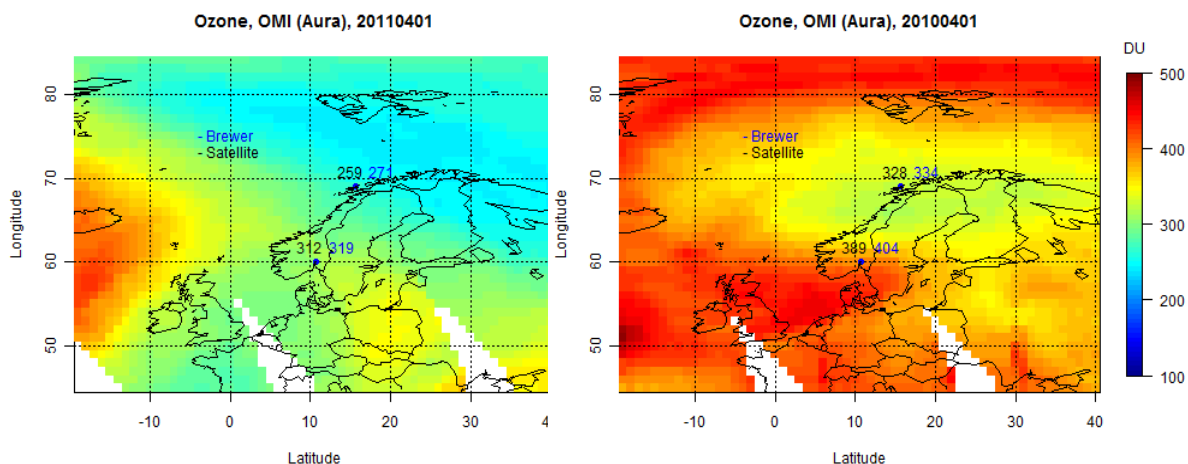


Figure 15: Ozone maps over Scandinavia and the Arctic 1st April 2011 (left panel) and 1st April 2010 (right panel). The numbers above Oslo and Andøya represent satellite observations (black) and ground based Brewer observation (blue numbers).

With respect to the monthly mean ozone values, there might be relatively large differences between the ground based measurements and the satellite data, and also between the various satellite data for overlapping time periods. There are both seasonal and systematic differences between the various satellite products.

The monthly mean ozone values from ground based (GB) measurements and satellites are analysed for the full period 1979-2011. Figure 16 shows the percentage GB-Satellite deviation at Oslo (upper panel) and at Andøya (lower panel) for different satellite products. Monthly mean ozone values are calculated from days where simultaneous ground based and satellite data are available. The most surprising finding is that the monthly mean deviation between the different satellite retrievals can be up to 15%, e.g. in December 2004 where OMI measured 328 DU and SCIAMACHY measured 380 DU, a difference of 52 DU. The ground based Brewer observation was 329 DU this month, which was close to the OMI ozone value.

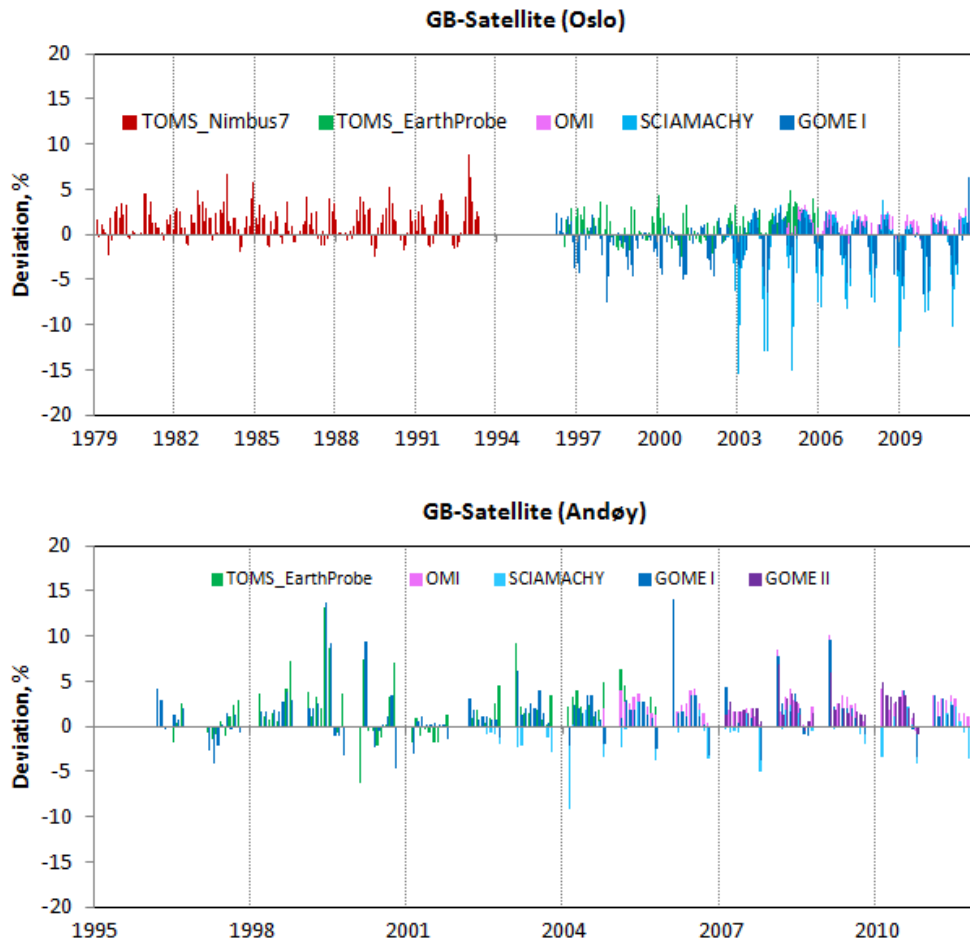


Figure 16: Difference between ground based (GB) and satellite retrieved monthly mean ozone values from 1979 to 2011 for Oslo and 1995-2011 for Andøya. Deviations (GB minus satellite values) are given in %. Upper panel: Oslo, Lower panel: Andøya.

Table 7 gives an overview of the average deviations between ground based ozone measurements and various satellite data products, together with standard deviations and variance for Oslo and Andøya. For Oslo, ozone retrieved from TOMS, OMI and GOME II seems to be slightly underestimated, whereas GOME I and SCIAMACHY tend to overestimate the ozone. For Andøya all mean satellite values are lower than the ground based observations. There are also clear seasonal variations in the deviations between GB ozone and satellite retrieved values, especially in Oslo. For example, SCIAMACHY systematically overestimates ozone values in December, January and February. This gives a very high standard deviation and variance for the GB-SCIAMACHY deviation in Oslo. The high SCIAMACHY winter values are visualized by the light blue columns/lines in Figure 16 (upper panel). In contrast the OMI ozone values are close to the Brewer measurements in Oslo all year, giving a variance of only 1.9 (see Table 7.). For Andøya the BG-SCIAMACHY variance is much smaller than in Oslo. This is probably caused by the fact that no measurements are performed in December, January and most of November and February. Thus, the months with largest uncertainty and variance are omitted from the comparison.

Table 7: Average deviations in % between ground based and satellite retrieved monthly mean ozone values from Oslo and Andøya. Standard deviation and variance are also included.

Oslo					
Instrument	Period		Mean	St. Dev	Variance
TOMS (Nimbus 7)	Nov-78	May-93	1.35	1.88	3.53
TOMS (Earth probe)	Jul-96	Dec-05	0.96	1.60	2.56
OMI	Oct-04	Dec-11	1.03	1.39	1.94
GOME I	Mar-96	Jul-11	-0.85	2.42	5.84
GOME II	Jan-07	Dec-11	1.22	1.42	2.00
SCIAMACHY	Jul-02	Dec-11	-2.03	4.42	19.54
Andøya					
Instrument	Period		Mean	St. Dev	Variance
TOMS (Earth probe)	Jul-96	Dec-05	1.71	2.86	8.18
OMI	Oct-04	Oct-11	2.67	2.20	4.82
GOME 1	Mar-96	Jul-11	1.42	2.78	7.74
GOME 2	Jan-07	Dec-11	2.16	1.55	2.41
SCIAMACHY	Jul-02	Dec-11	0.30	2.37	5.62

One aim of the SatLuft and SatMonAir project is to define and construct an integrated satellite data set that is suitable for trend analysis for the Scandinavian region. Based on the analysis and results presented in Table 7 it seems like the ozone data from TOMS and OMI have similar mean and standard deviation and are most suited for further trend studies, especially in southern Norway. However, a series of new satellite retrieval versions will also be investigated before any conclusions are drawn.



Norwegian Institute
for Air Research

NILU – Norwegian Institute for Air Research
P.O. Box 100, N-2027 Kjeller, Norway
Associated with CIENS and the Fram Centre
ISO certified according to NS-EN ISO 9001/ISO 14001

REPORT SERIES SCIENTIFIC REPORT	REPORT NO. OR 46/2013	ISBN: 978-82-425-2617-5 (print) 978-82-425-2618-2 (electronic) ISSN: 0807-7207	
DATE 10/12/2013	SIGN. 	NO. OF PAGES 69	PRICE NOK 150.-
TITLE Towards operational satellite based atmospheric monitoring in Norway SatMoNAir Final project report		PROJECT LEADER Aasmund Fahre Vik	
		NILU PROJECT NO. O-111154	
AUTHOR(S) Kerstin Stebel, Aasmund Fahre Vik, Cathrine Lund Myhre, Ann Mari Fjæraa, Tove Svendby and Phillip Schneider		CLASSIFICATION * A	
		CONTRACT REF. JOP.12.12.2	
QUALITY CONTROLLER: Tove Svendby			
REPORT PREPARED FOR Norwegian Space Centre P.O.Box 113 Skøyen 0212 Oslo			
ABSTRACT The SatMoNAir project [NSC contract nr. JOP.12.12.2] builds on a previous NRS 'følgemiddel'-project, called 'Roadmap towards EarthCARE and Sentinel 5 precursor', within which NILU and met.no developed a strategy for how best to prepare themselves for future European satellite missions for measuring atmospheric composition, with respect to their national monitoring, weather predictions and research tasks. Three specific topics were considered particularly relevant: a. Aerosols – Climate effects in Scandinavia and polar regions: analysis of episodes with high aerosol loads for Klif reporting, b. the Use of satellite based ozone measurements in national reporting, and c. Satellite based Air Quality monitoring of remote areas for EMEP reporting. Results from the work performed are described in this report. The outcomes of the project have been utilized in support of the National monitoring of greenhouse gases and aerosols (see Myhre et al., 2012), the atmospheric ozone layer (see Svendby et al., 2012), and have been reported to EMEP.			
NORWEGIAN TITLE Mot operasjonell satellittbasert atmosfæreovervåkning i Norge – SatMoNAir			
KEYWORDS	Earth Observation	Aerosols, CO, ozone, NO ₂	Monitoring
ABSTRACT (in Norwegian) SatMoNAir prosjektet [NSC kontrakt nr. JOP.12.12.2] bygger på et tidligere NRS følgemiddelprosjekt kalt "Roadmap towards EarthCARE and Sentinel 5 precursors", der NILU og met.no utviklet en strategi for å være forberedt på framtidige satellittobservasjoner knyttet til nasjonal klimaovervåkning, værvarsel og forskning. Det har blitt fokusert på tre områder: a. Aerosol- klimaeffekter i Skandinavia og polare strøk, b. Bruk av satellitter i nasjonal overvåkning av ozonlaget, c. Satellittbaserte målinger av luftkvalitet til bruk i EMEP rapportering. Resultater fra dette arbeidet blir beskrevet i denne rapporten. Prosjektet har vært en viktig støtte for NILUs nasjonale overvåkning av klimagasser og aerosoler (Myhre et al., 2012) og atmosfærens ozonlag (Svendby et al., 2012). Resultater har også blitt rapportert til EMEP.			

* Classification
A Unclassified (can be ordered from NILU)
B Restricted distribution
C Classified (not to be distributed)

REFERENCE: O-111154
DATE: DECEMBER 2013
ISBN: 978-82-425-2617-5 (print)
978-82-425-2618-2 (electronic)

NILU – Norwegian Institute for Air Research is an independent, nonprofit institution established in 1969. Through its research NILU increases the understanding of climate change, of the composition of the atmosphere, of air quality and of hazardous substances. Based on its research, NILU markets integrated services and products within analyzing, monitoring and consulting. NILU is concerned with increasing public awareness about climate change and environmental pollution.